Dataset for Photo Response of ^{150}Nd: Experimental Spectra

Supplementary Material to "Exploration of Nuclear-Structure Effects on Averaged Decay Quantities in the Quasicontinuum

Oliver Papst

June 25, 2024

TECHNISCHE
UNIVERSITÄT
DARMSTADT

Department of Physics
Institut für Kernphysik
AG Pietralla

Contents

List of Figures

1 Spectra and fits of average decay branches of ^{150}Nd

The figures in this section show the fits used to analyze the contributions from different decay channels to the measured spectra. For each beam energy, a single fit is performed that simultaneously takes into account all spectra from all available detectors. This includes the 0°-detector which is not depicted but used to determine the energy shape of the LCB photon beam.

The fit result should be able to reproduce the measured spectrum as closely as possible, excluding statistical fluctuations. The fit yields a decomposition into the individual contributions to each spectrum. This includes the measurement of the decay of excited states to the ground state 0_1^+ and the first excited state 2_1^+. Also, the figures depict a decomposition into contributions from states with different parity, distinguishing between the possible decay channels $0_1^+ \rightarrow 1_{ex}^+ \rightarrow 0_1^+$, $0_1^+ \rightarrow 1_{ex}^- \rightarrow 0_1^+$, $0_1^+ \rightarrow 1_{ex}^+ \rightarrow 2_1^+$, and $0_1^+ \rightarrow 1_{ex}^- \rightarrow 2_1^+$.

Additionally, contributions from natural background radiation and radiation caused by atomic scattering of the photon beam on the target are shown. Finally, for some runs, NRF reactions on 2^+ states of ^{12}C and ^{16}O result in additional contributions.

The reproduction of the original spectrum is obtained by convoluting the contributions with the corresponding detector-response matrix (excluding the natural background radiation, which is added separately). To obtain a representation of each contribution that is scaled to the measured spectrum (i.e., includes the detection efficiency but no escape peaks or Compton continuum), the spectra are multiplied with the diagonal of the detector-response matrix.

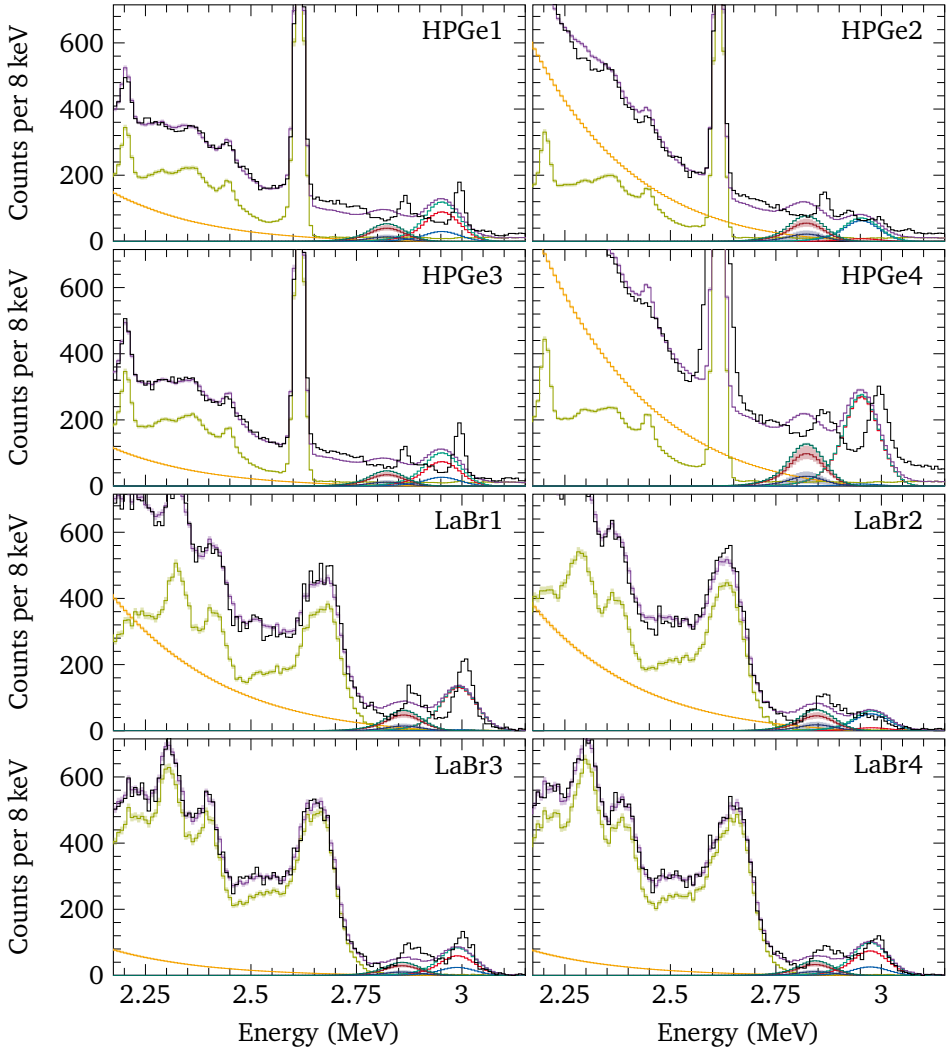

Figure 1.1: Fit of average decay branches of ^{150}Nd for $E_{\text{beam}} = 2.95\,\text{MeV}$

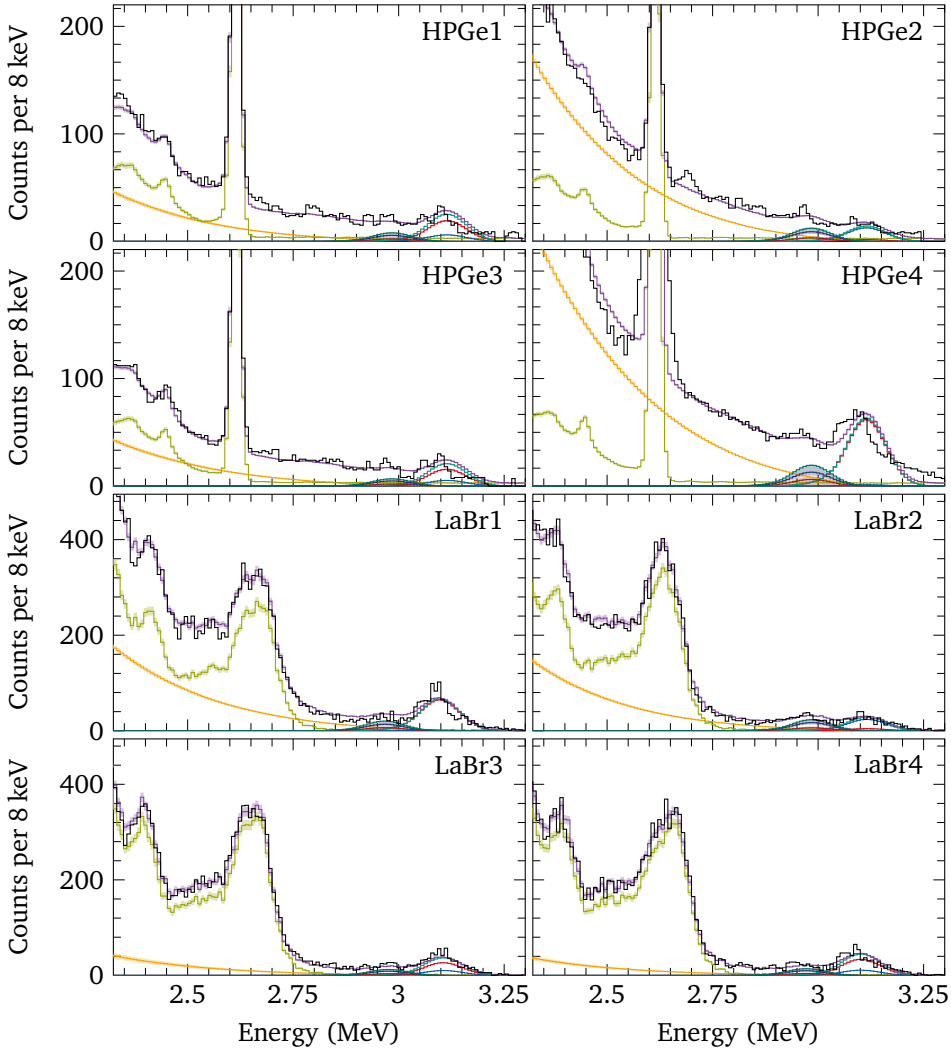

Figure 1.2: Fit of average decay branches of ^{150}Nd for $E_{\text{beam}} = 3.1\,\text{MeV}$

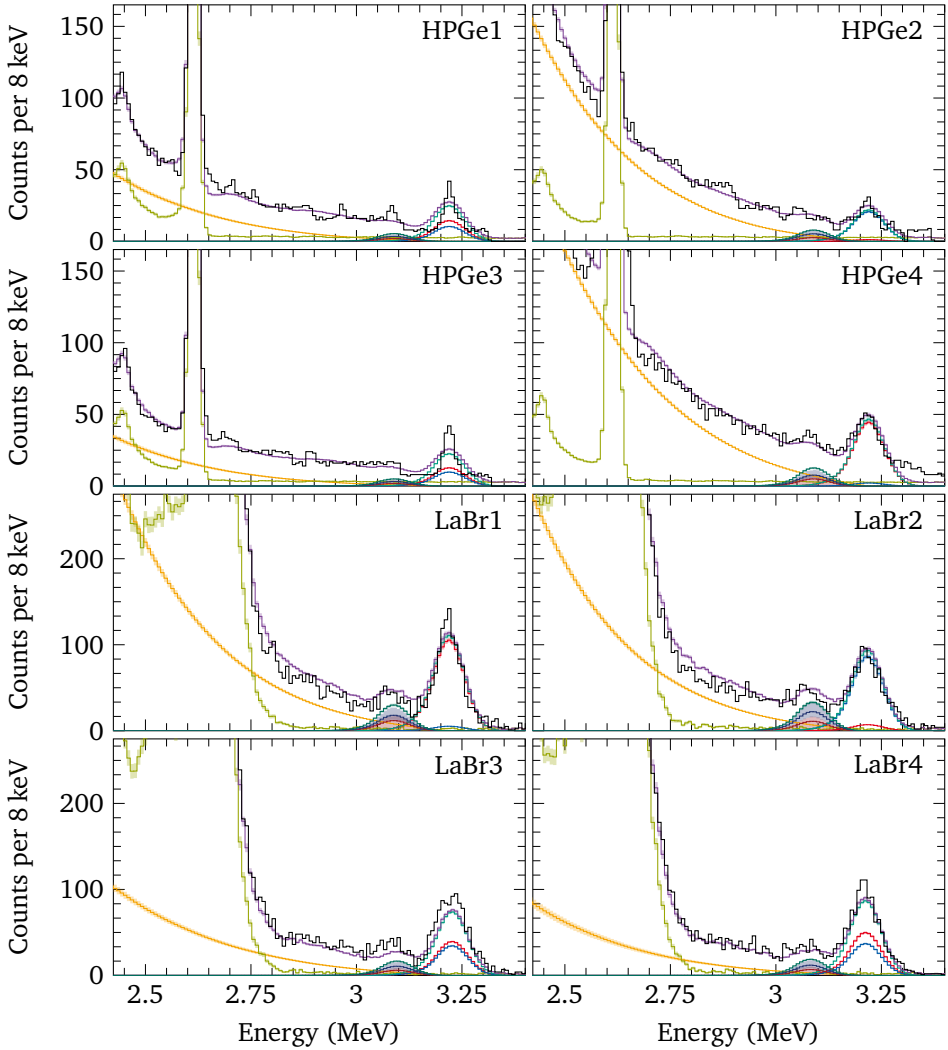

Figure 1.3: Fit of average decay branches of ^{150}Nd for $E_{\text{beam}} = 3.2\,\text{MeV}$

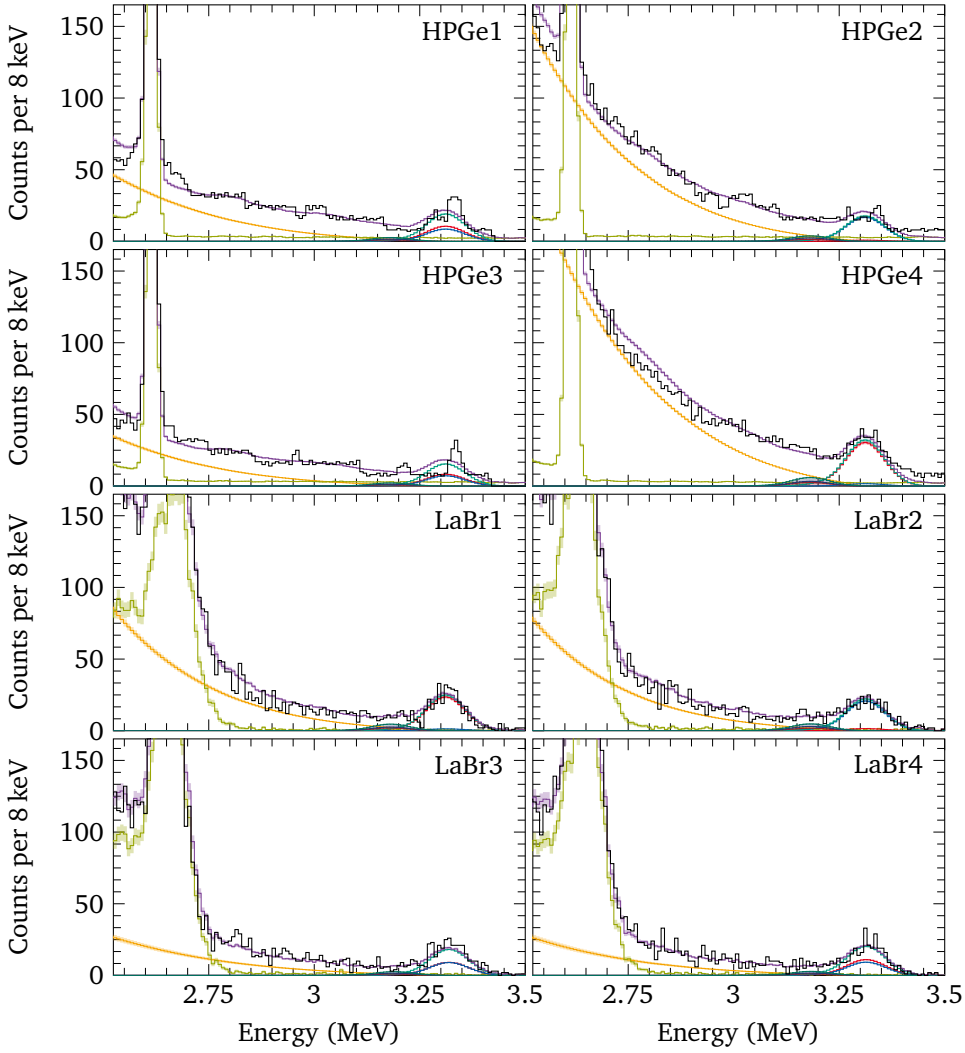

Figure 1.4: Fit of average decay branches of ^{150}Nd for $E_{\text{beam}} = 3.3\,\text{MeV}$

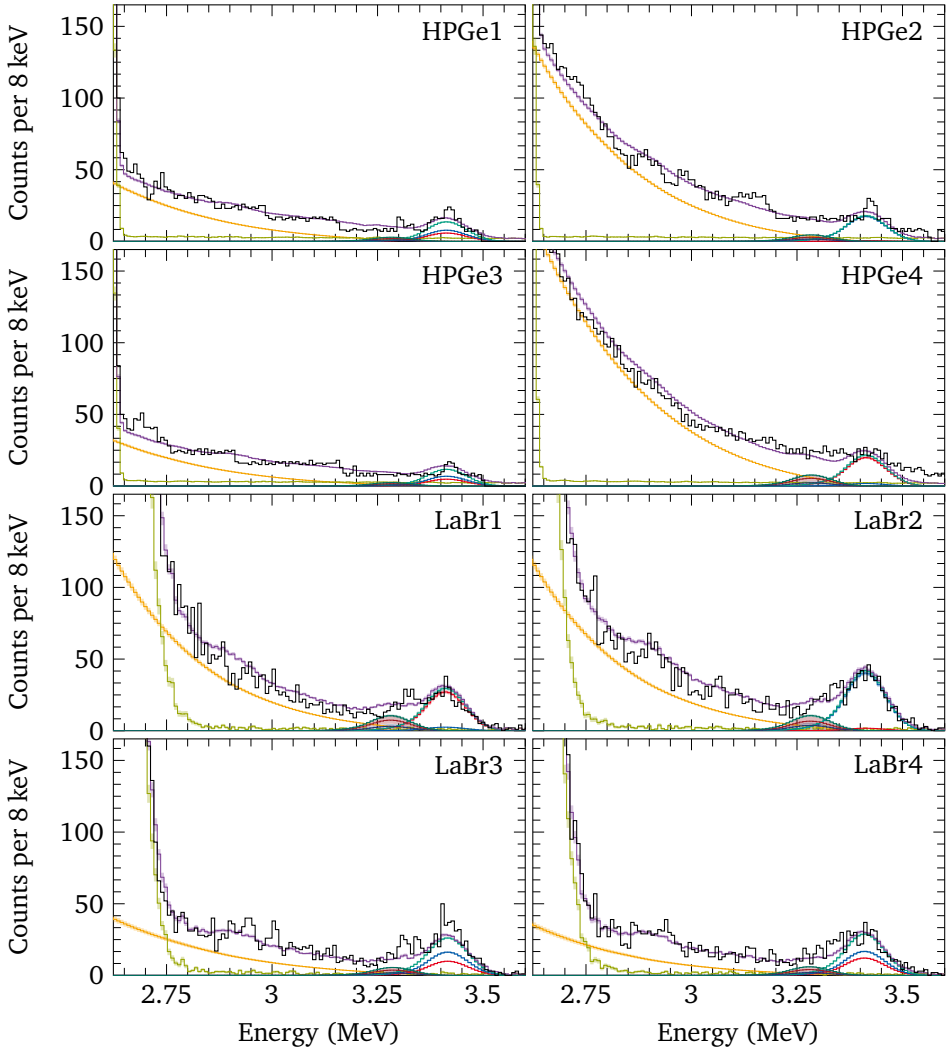

Figure 1.5: Fit of average decay branches of ^{150}Nd for $E_{\text{beam}} = 3.4\,\text{MeV}$

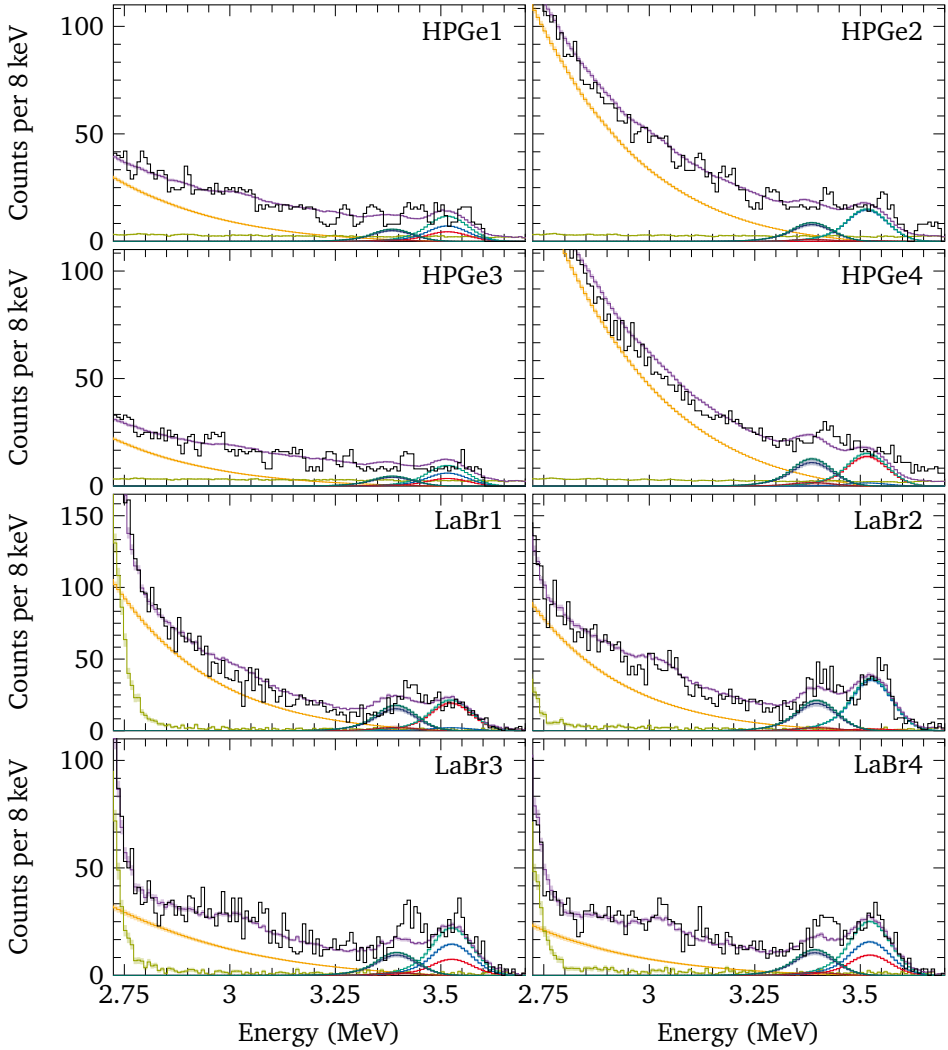

Figure 1.6: Fit of average decay branches of ^{150}Nd for $E_{\text{beam}} = 3.5\,\text{MeV}$

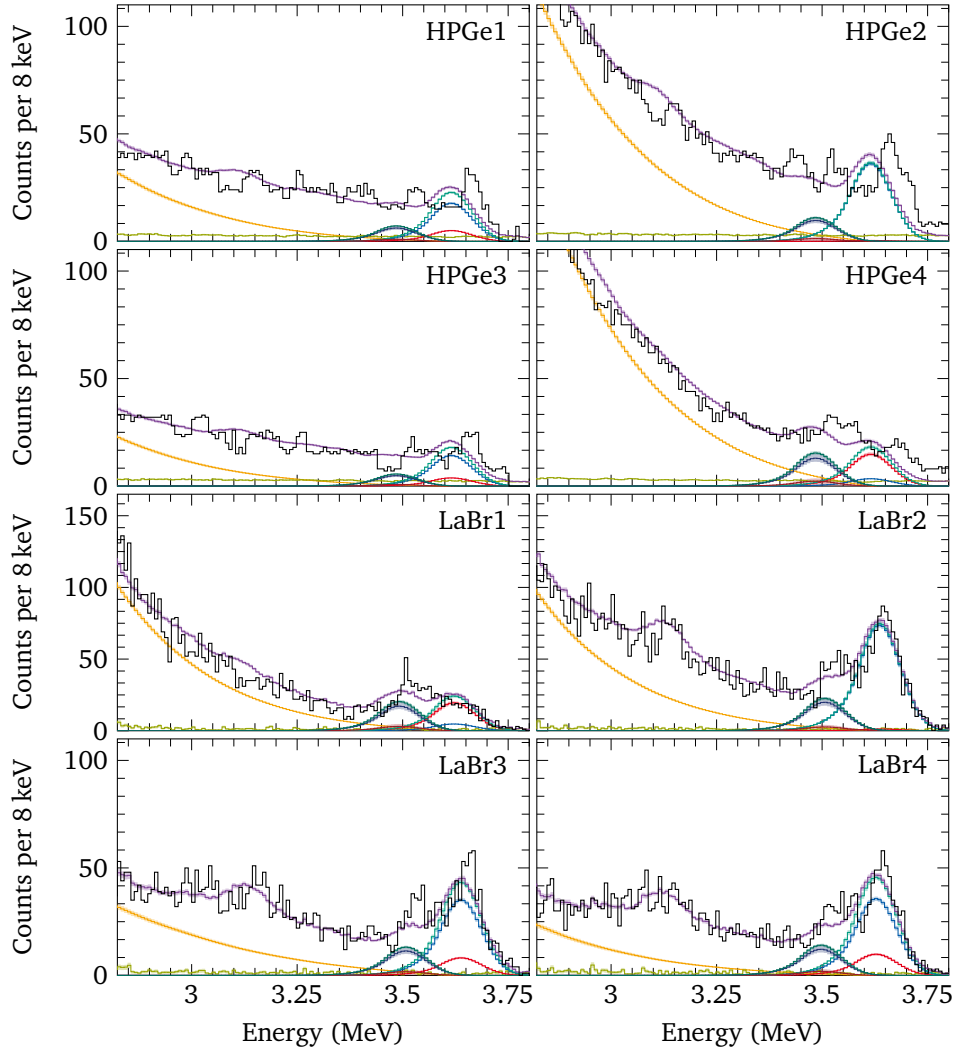

Figure 1.7: Fit of average decay branches of ^{150}Nd for $E_{\text{beam}} = 3.6\,\text{MeV}$

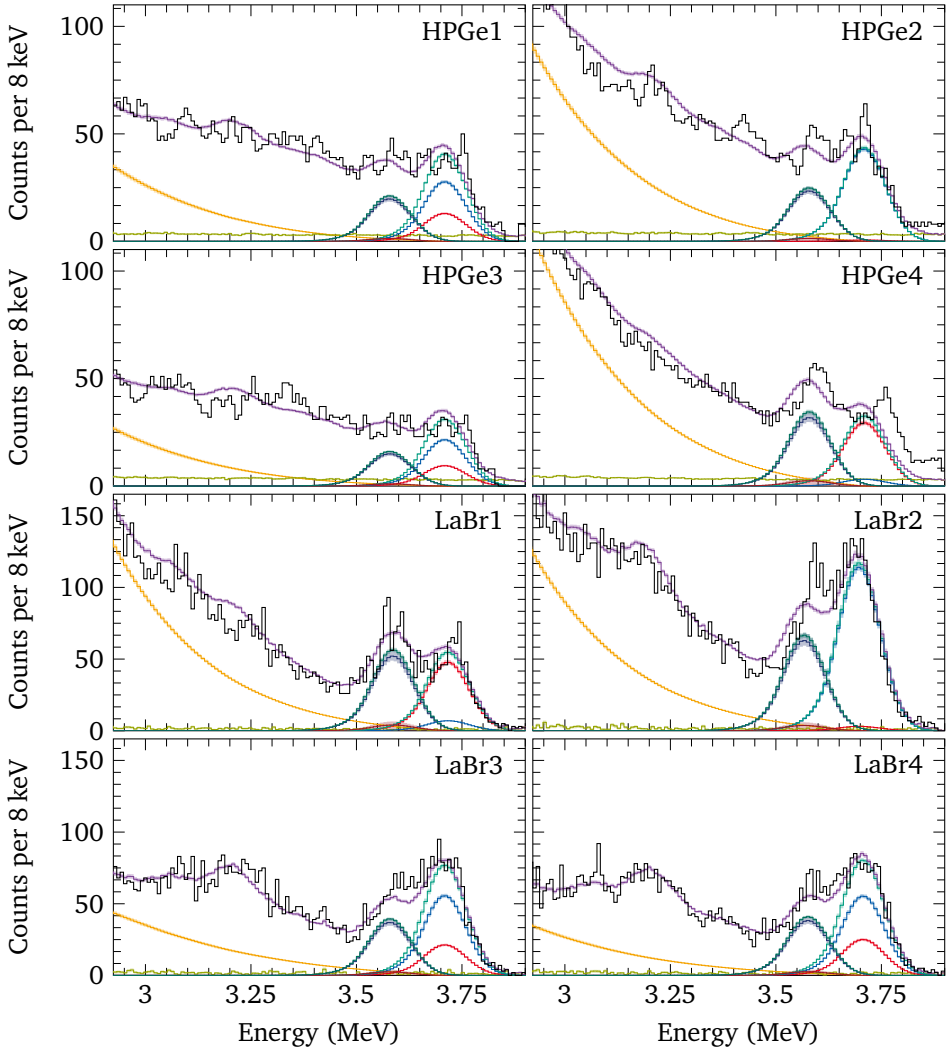

Figure 1.8: Fit of average decay branches of ^{150}Nd for $E_{\text{beam}} = 3.7\,\text{MeV}$

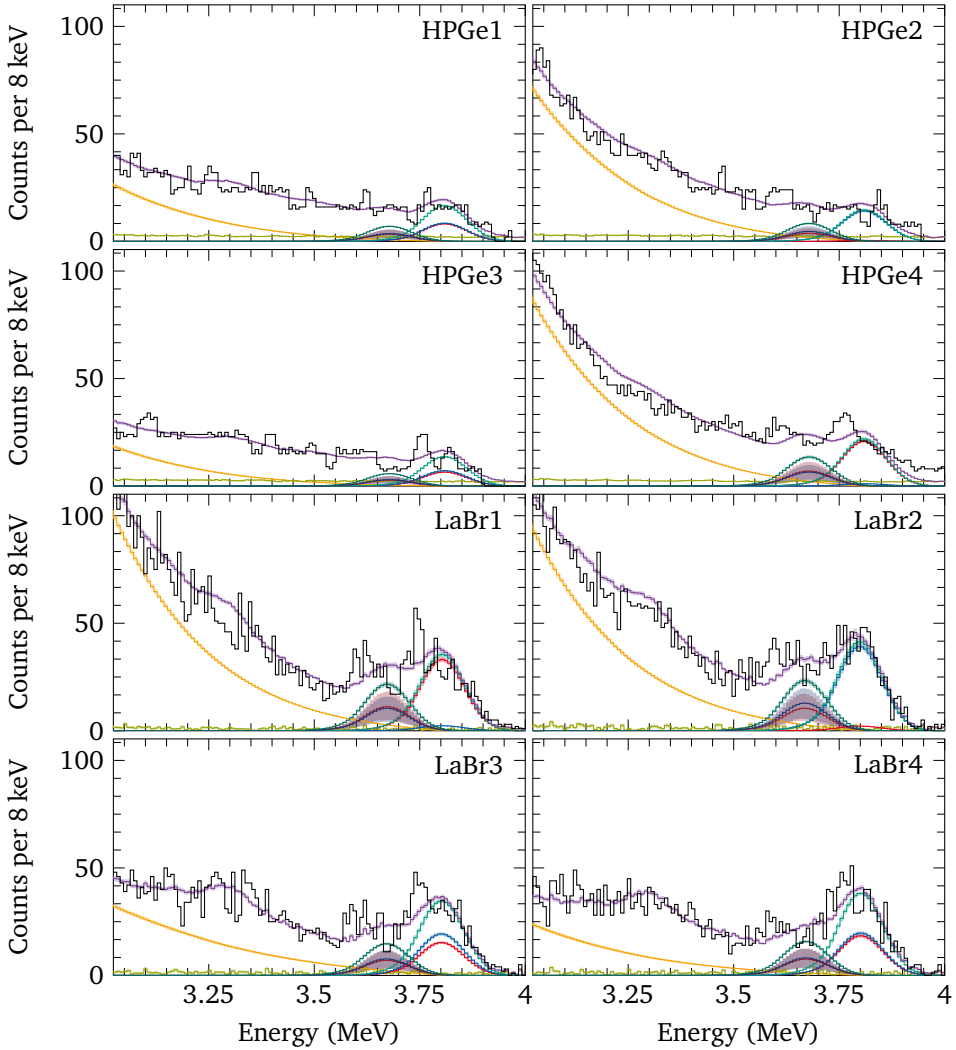

Figure 1.9: Fit of average decay branches of ^{150}Nd for $E_{\text{beam}} = 3.8\,\text{MeV}$

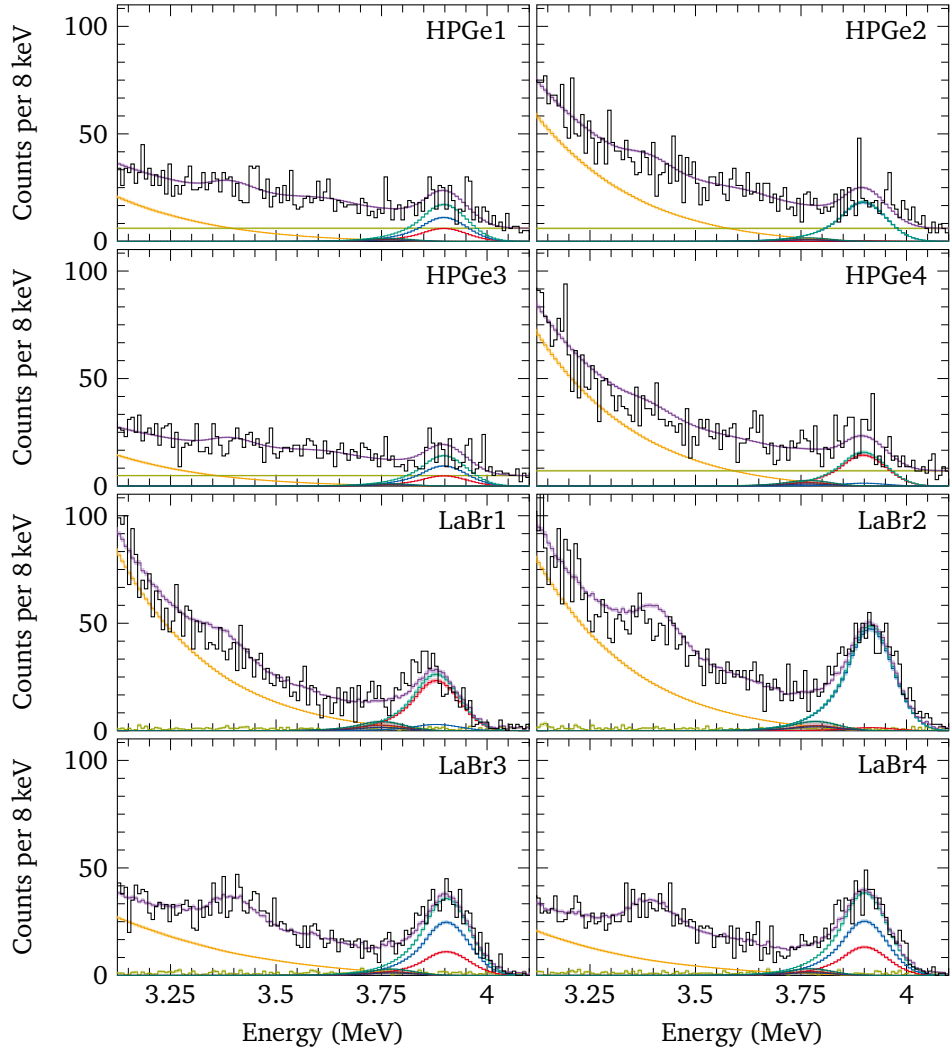

Figure 1.10: Fit of average decay branches of ^{150}Nd for $E_{\text{beam}} = 3.9\,\text{MeV}$

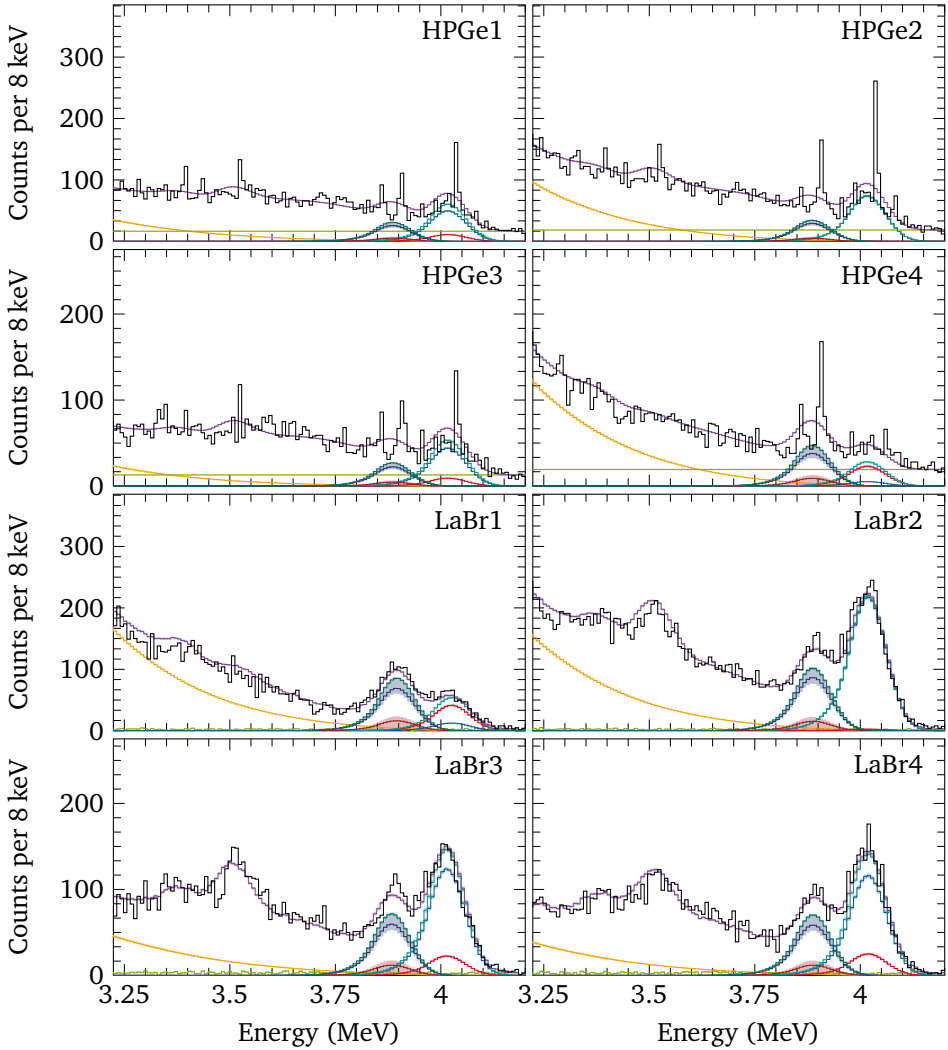

Figure 1.11: Fit of average decay branches of ^{150}Nd for $E_{\text{beam}} = 4.0\,\text{MeV}$

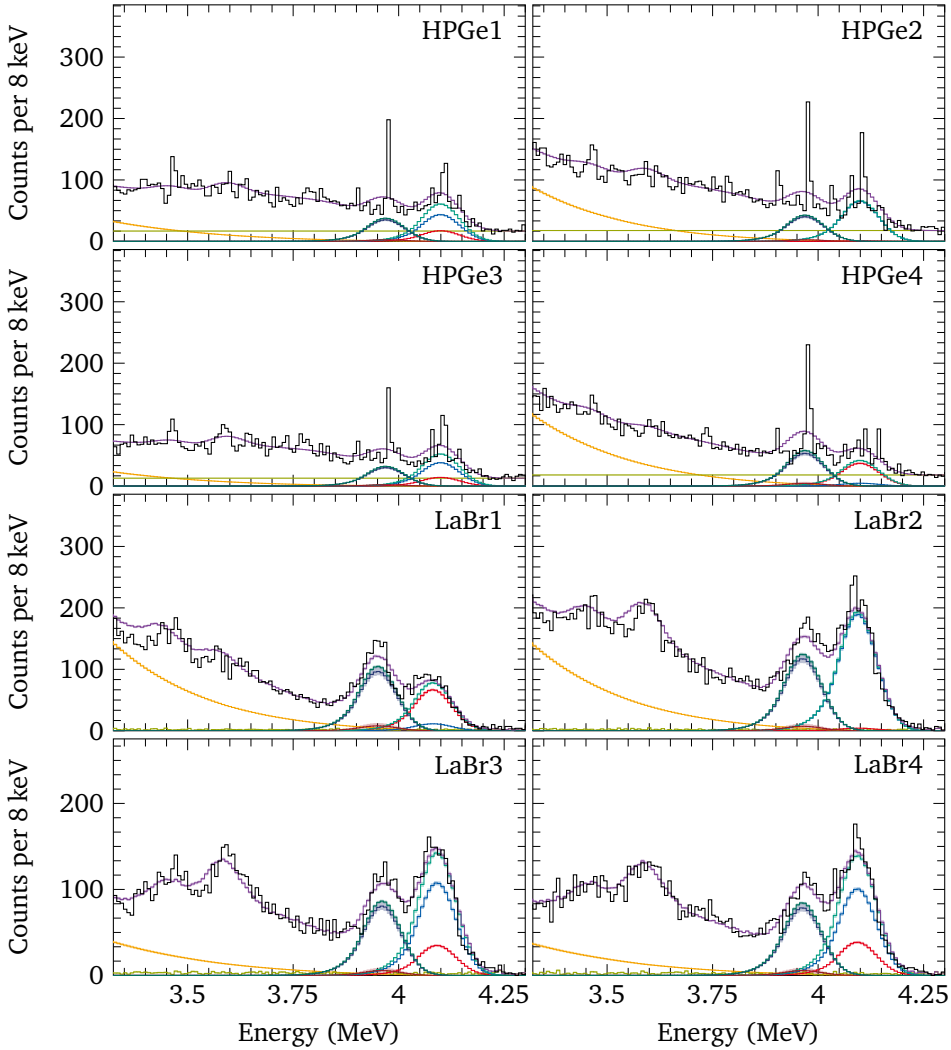

Figure 1.12: Fit of average decay branches of ^{150}Nd for $E_{\text{beam}} = 4.1\,\text{MeV}$

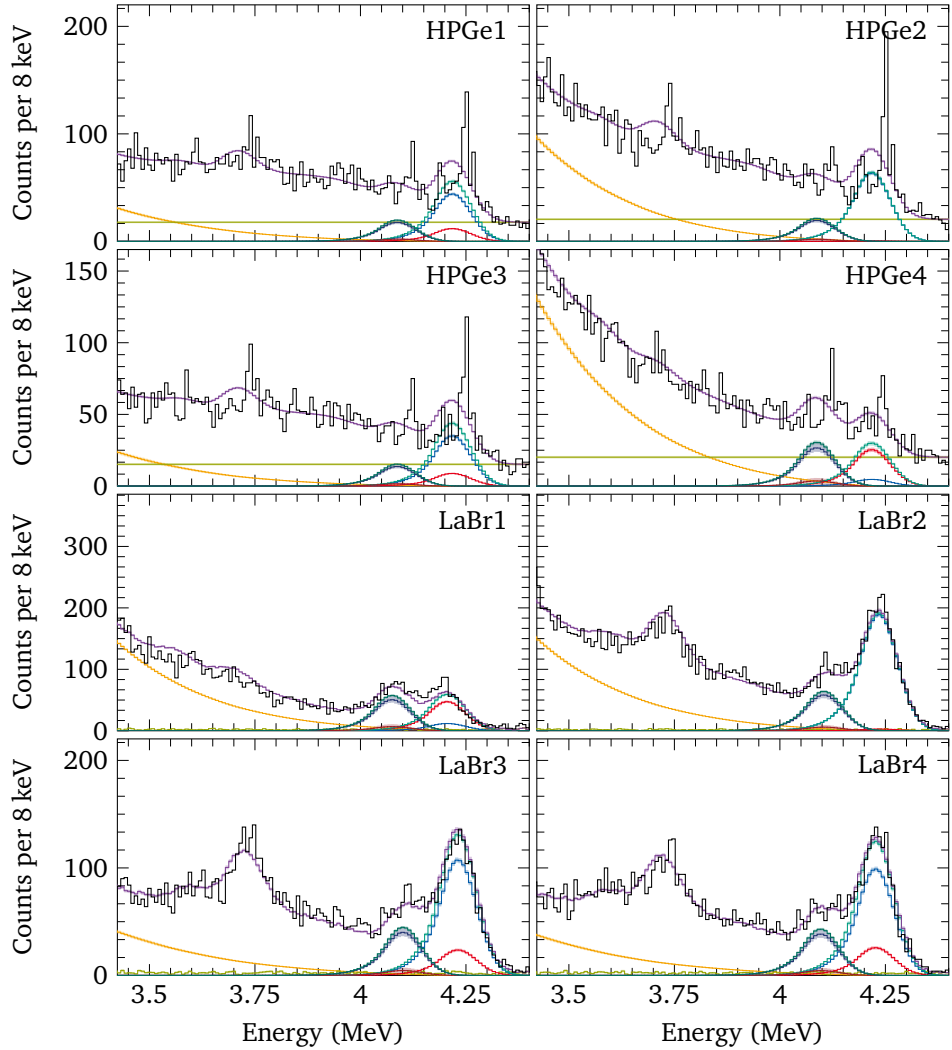

Figure 1.13: Fit of average decay branches of ^{150}Nd for $E_{\text{beam}} = 4.2\,\text{MeV}$

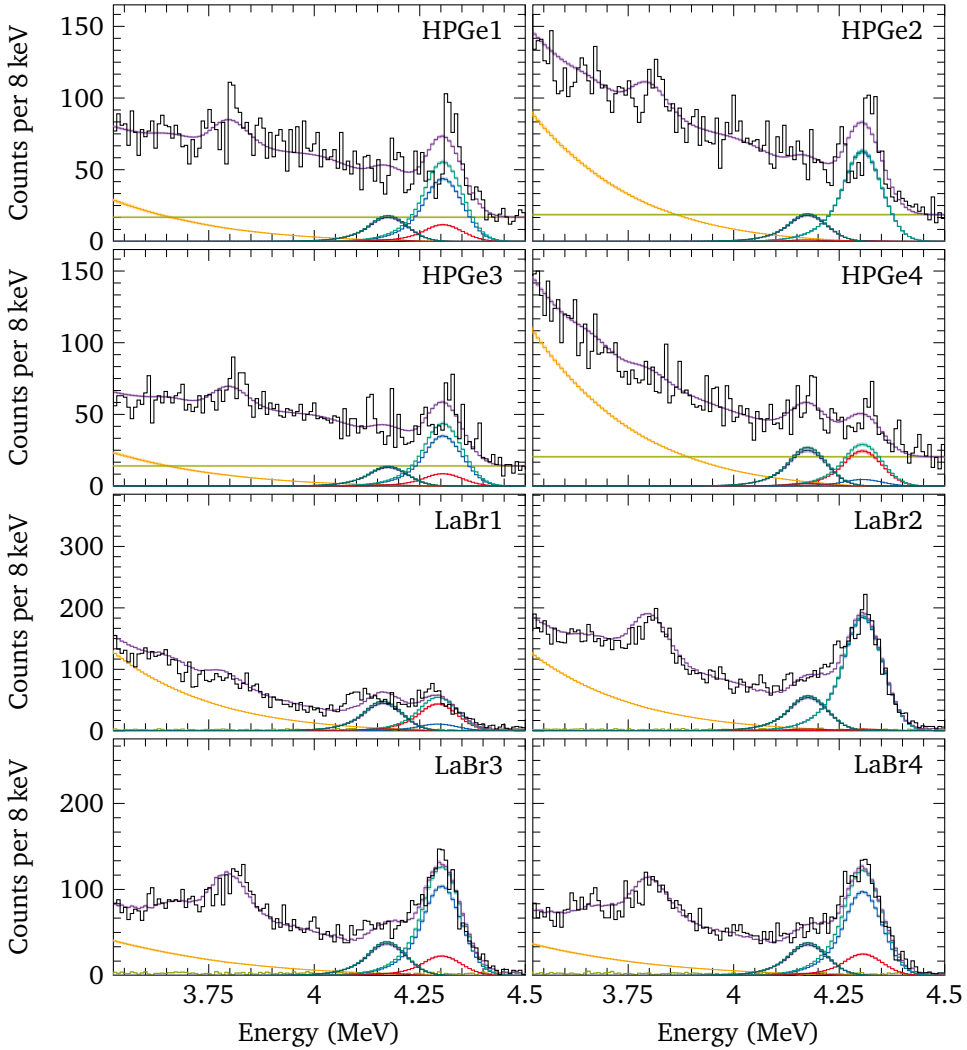

Figure 1.14: Fit of average decay branches of ^{150}Nd for $E_{\text{beam}} = 4.3\,\text{MeV}$

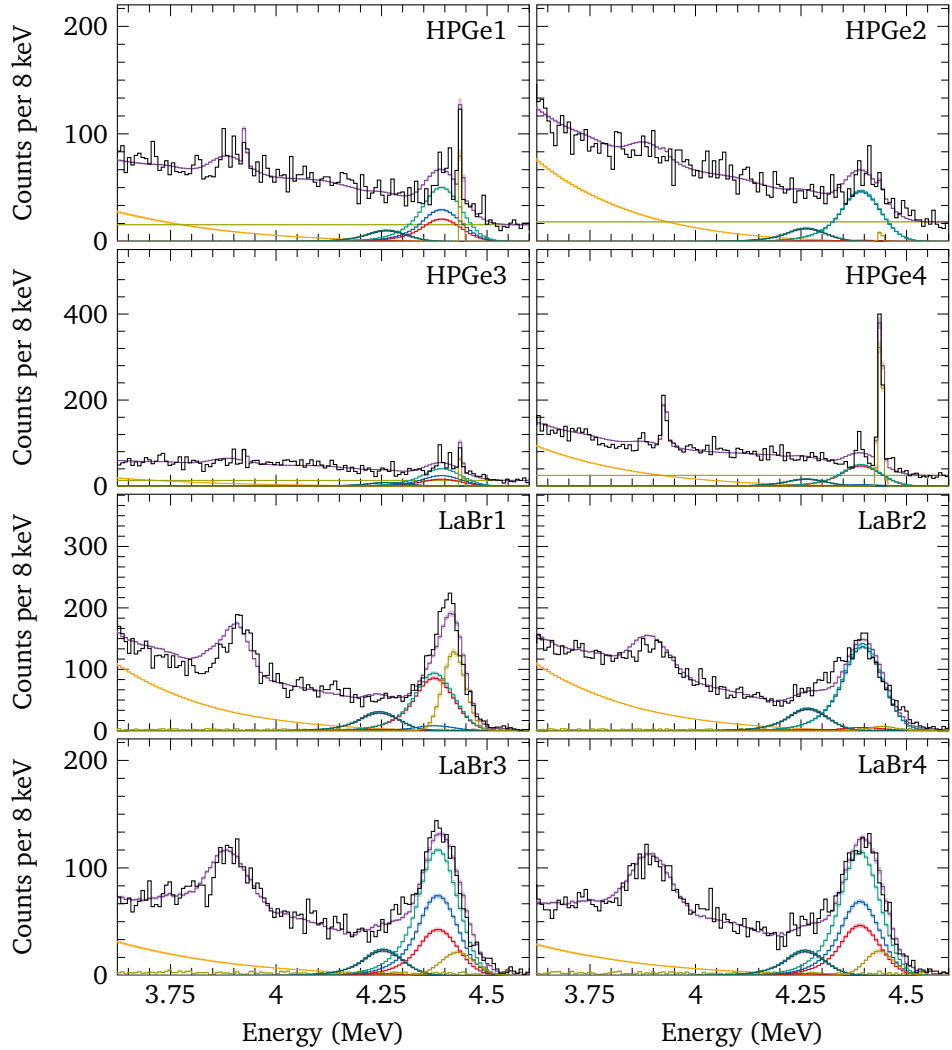

Figure 1.15: Fit of average decay branches of ^{150}Nd for $E_{\text{beam}} = 4.4\,\text{MeV}$

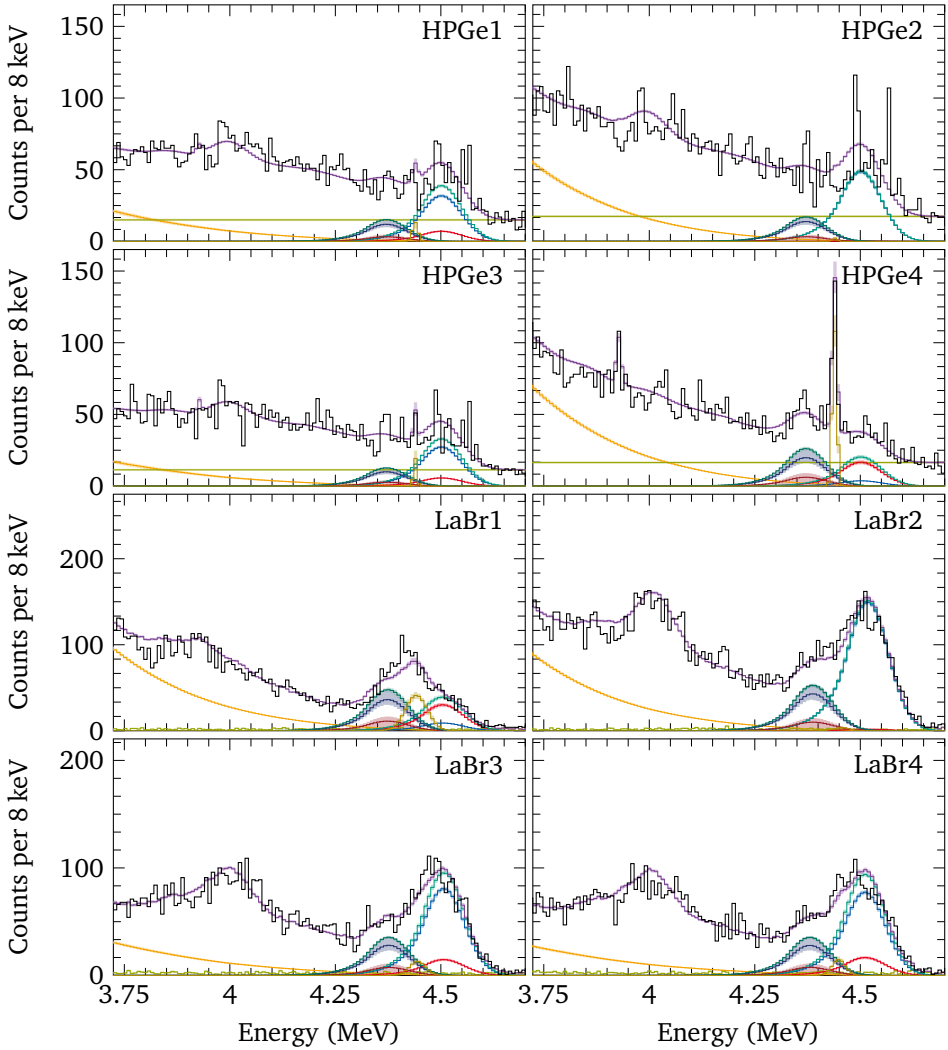

Figure 1.16: Fit of average decay branches of ^{150}Nd for $E_{\text{beam}} = 4.5\,\text{MeV}$

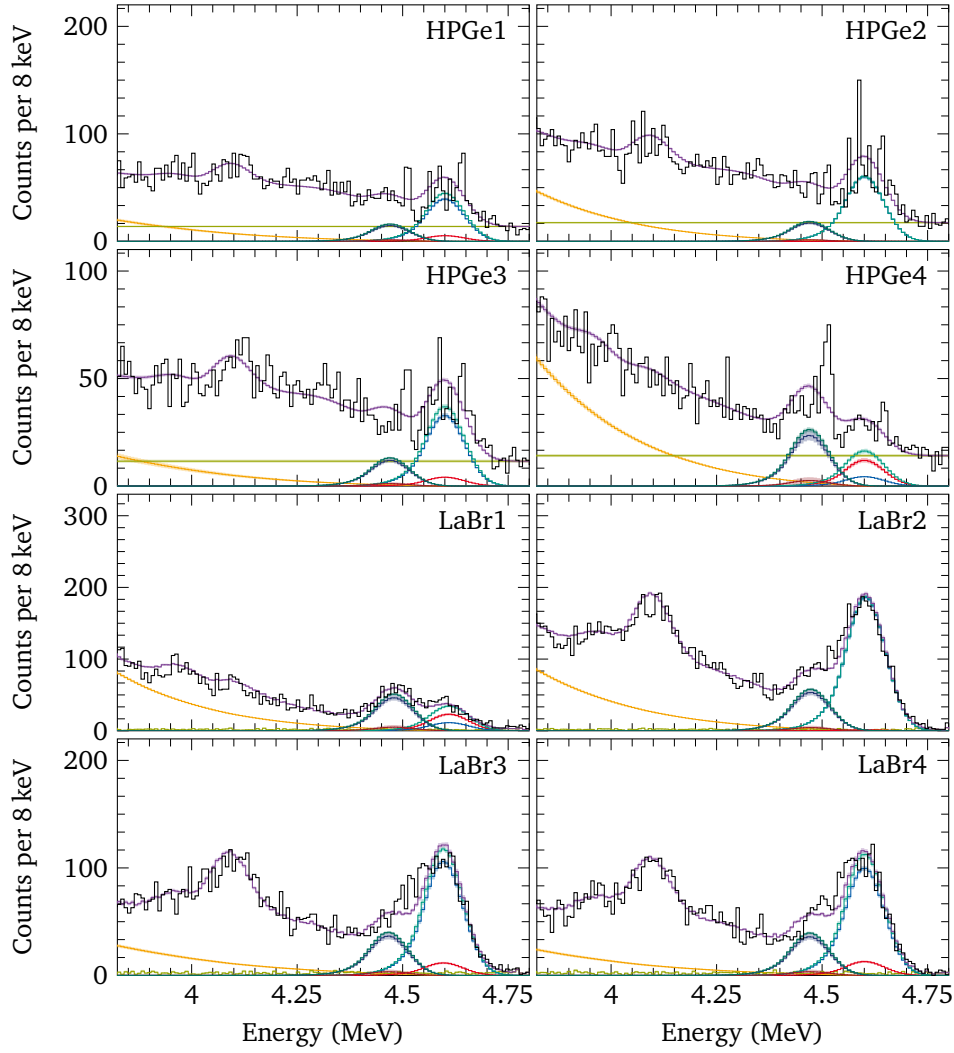

Figure 1.17: Fit of average decay branches of ^{150}Nd for $E_{\text{beam}} = 4.6\,\text{MeV}$

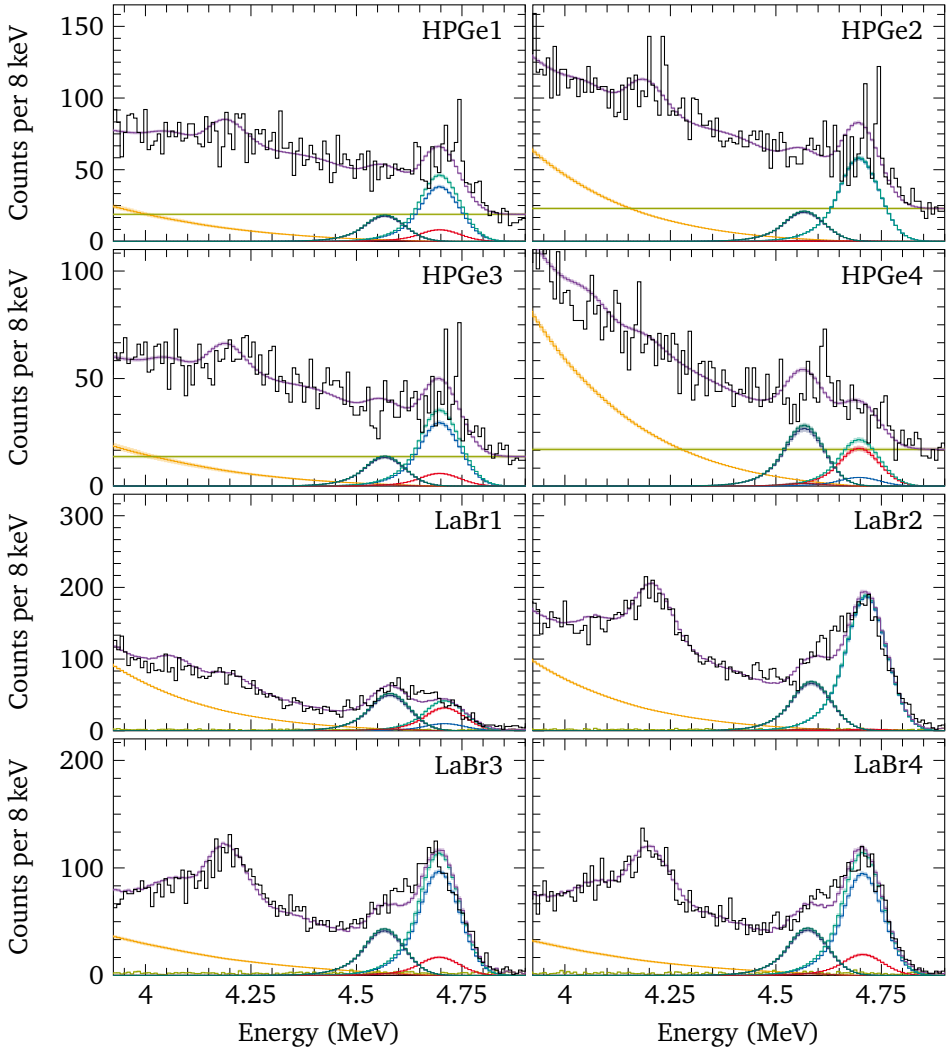

Figure 1.18: Fit of average decay branches of ^{150}Nd for $E_{\text{beam}} = 4.7\,\text{MeV}$

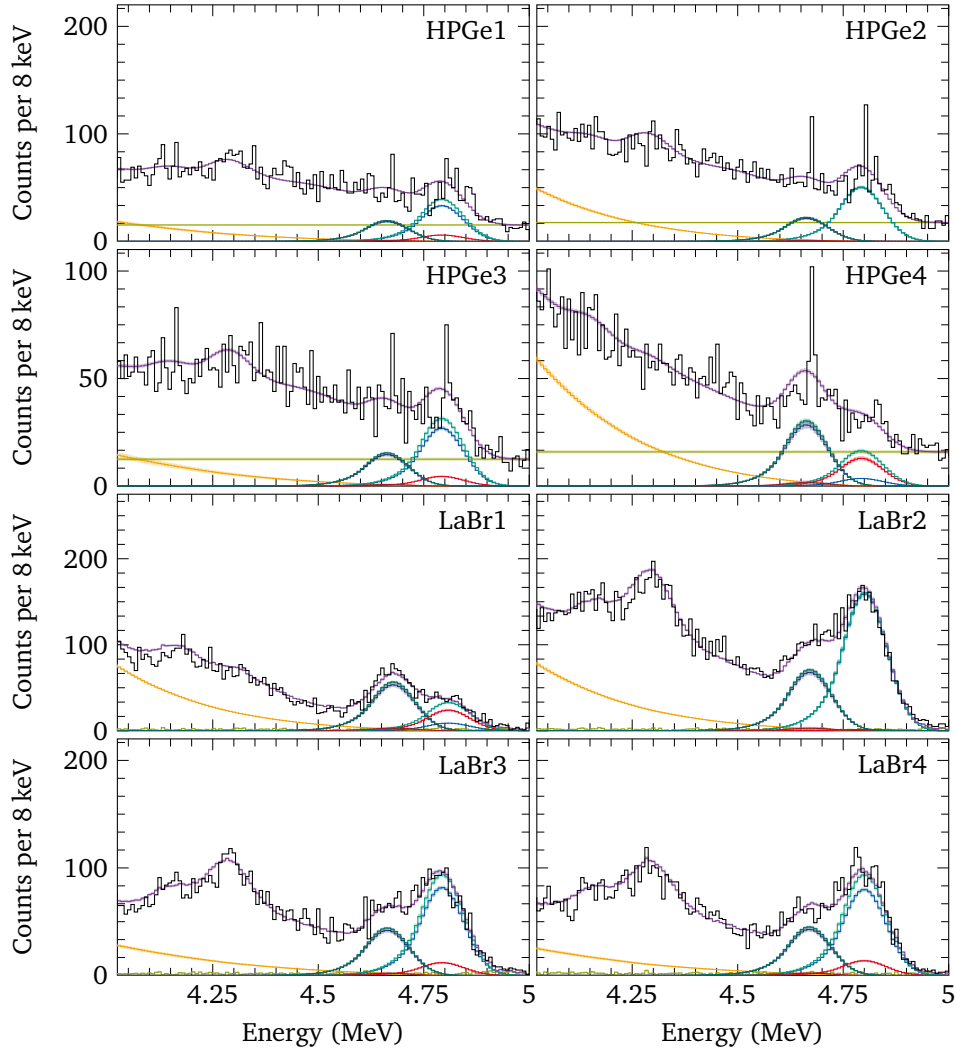

Figure 1.19: Fit of average decay branches of ^{150}Nd for $E_{\text{beam}} = 4.8\,\text{MeV}$

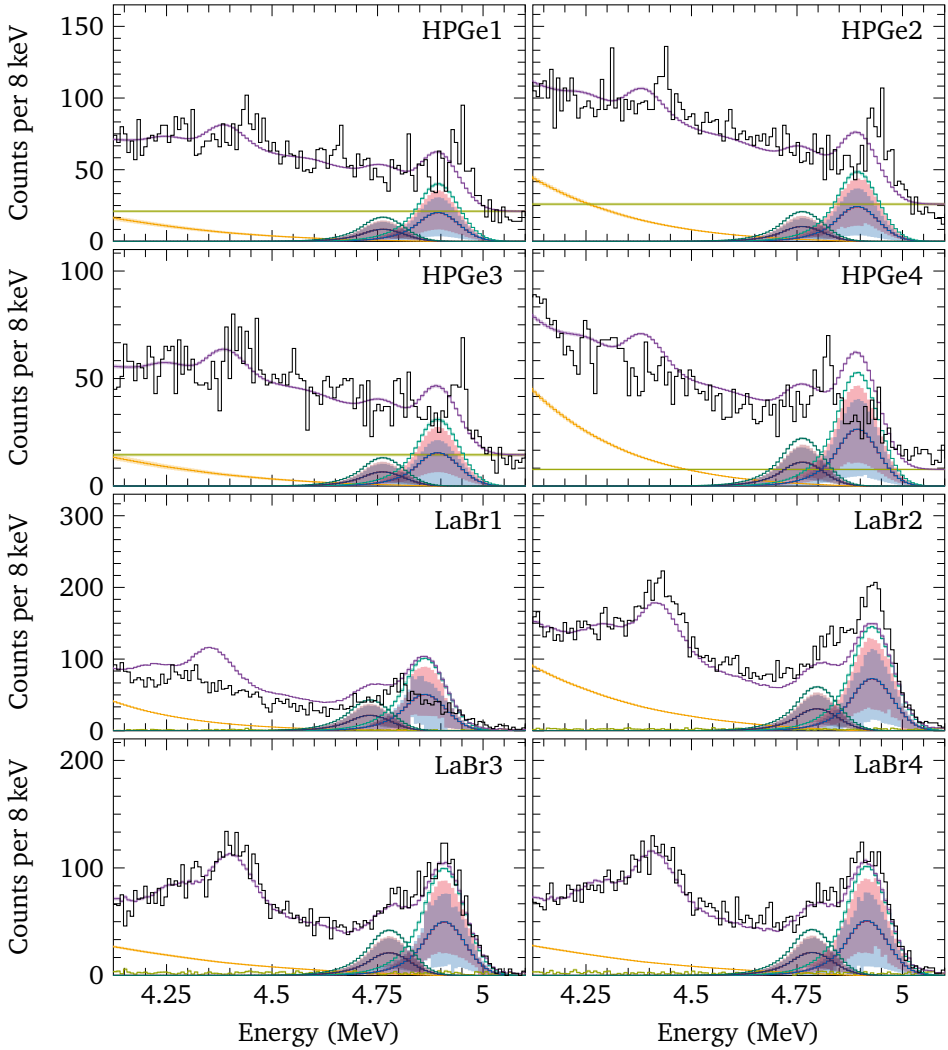

Figure 1.20: Fit of average decay branches of ^{150}Nd for $E_{\text{beam}} = 4.9\,\text{MeV}$

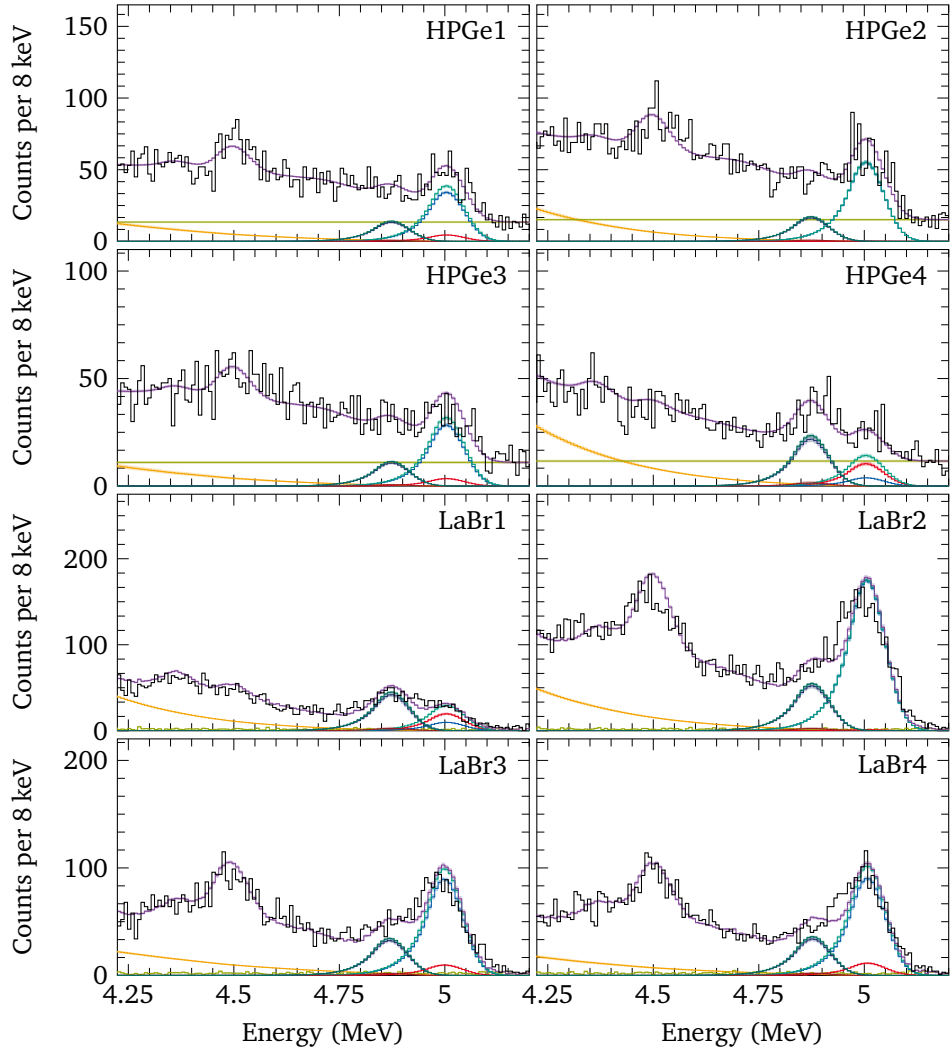

Figure 1.21: Fit of average decay branches of ^{150}Nd for $E_{\text{beam}} = 5.0\,\text{MeV}$

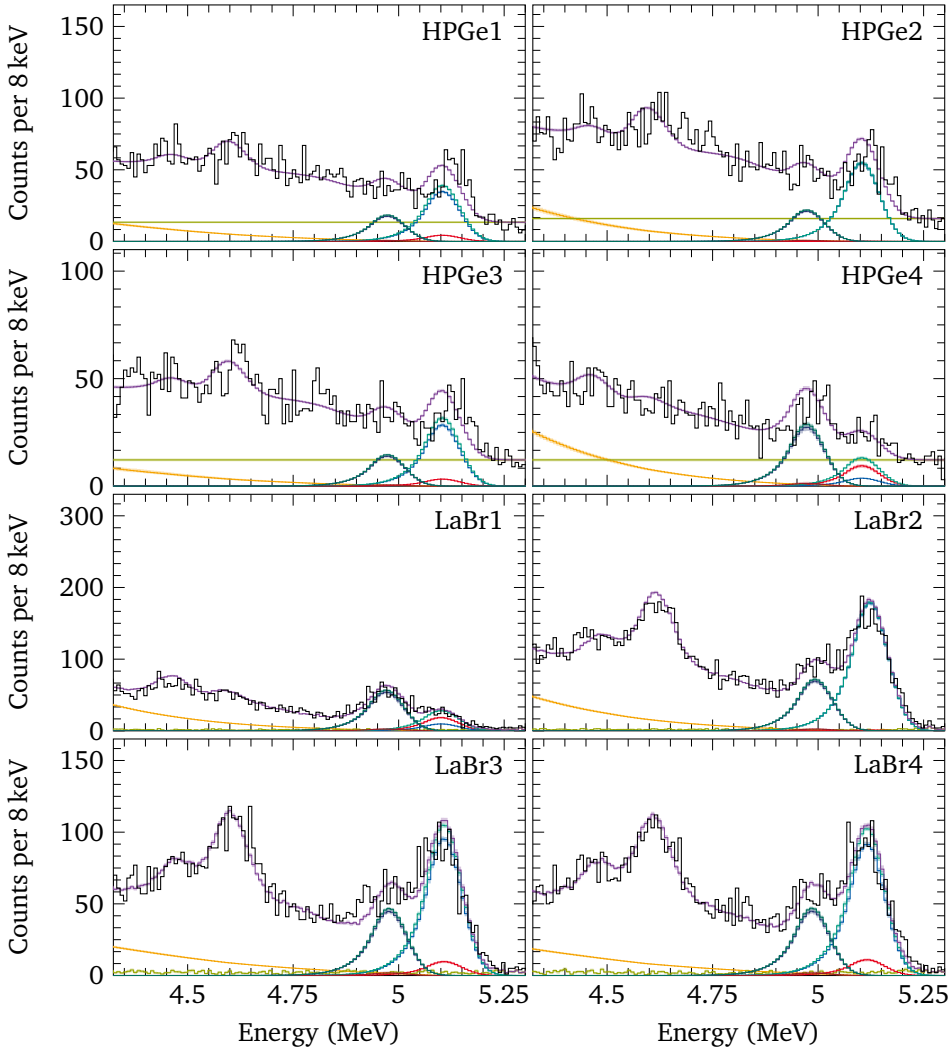

Figure 1.22: Fit of average decay branches of ^{150}Nd for $E_{\text{beam}} = 5.1\,\text{MeV}$

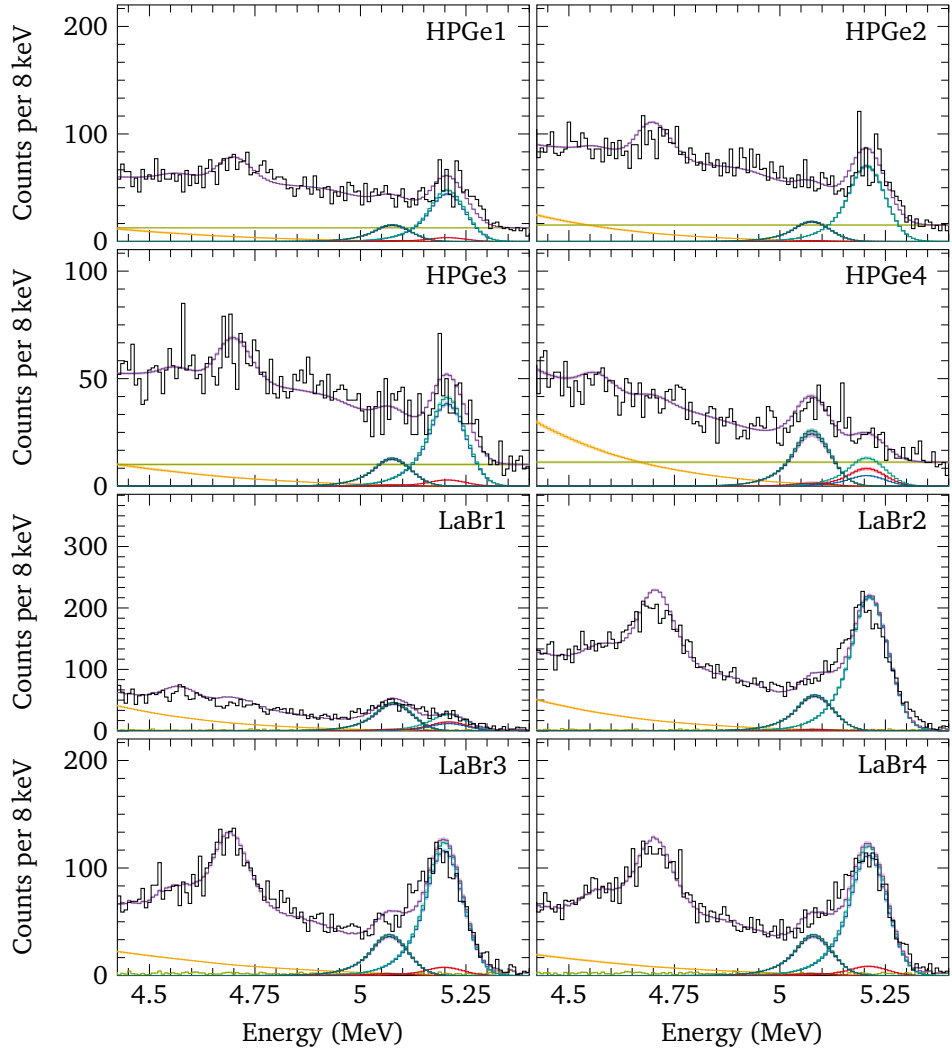

Figure 1.23: Fit of average decay branches of ^{150}Nd for $E_{\text{beam}} = 5.2\,\text{MeV}$

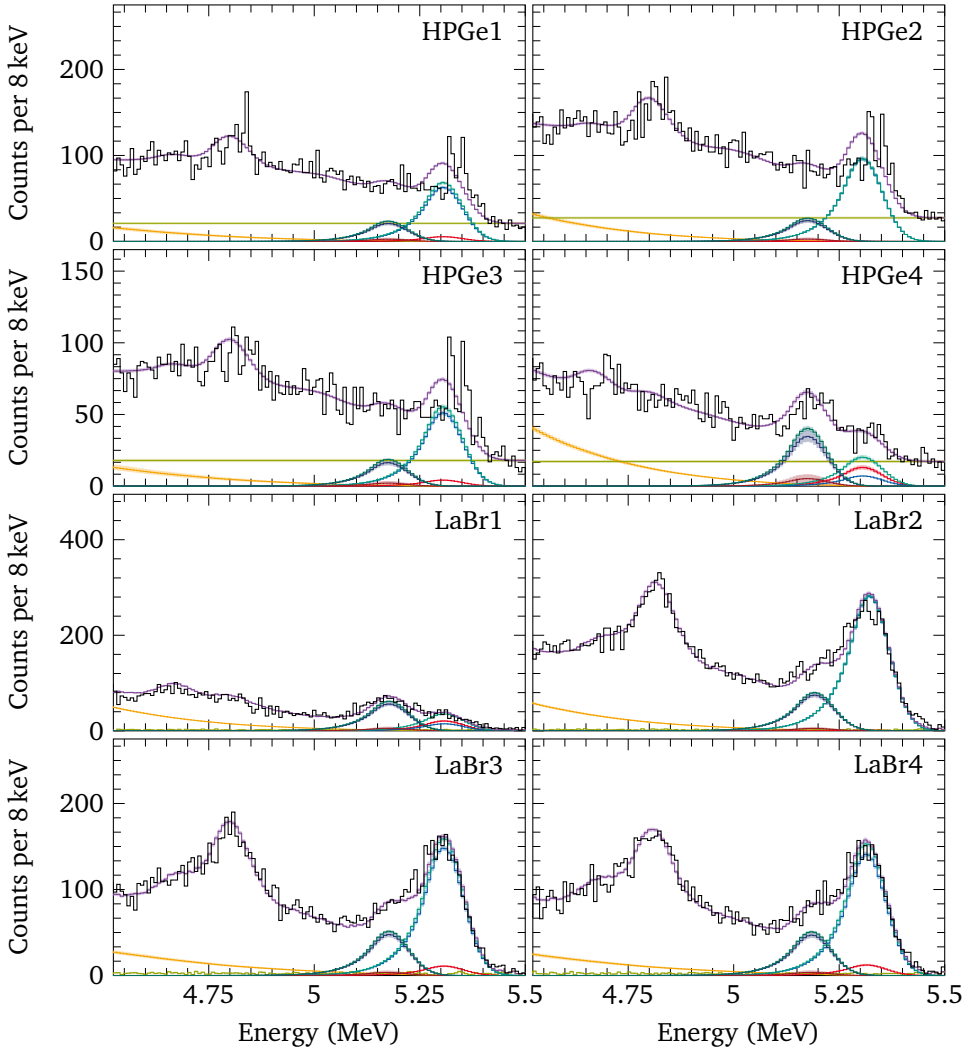

Figure 1.24: Fit of average decay branches of ^{150}Nd for $E_{\text{beam}} = 5.3\,\text{MeV}$

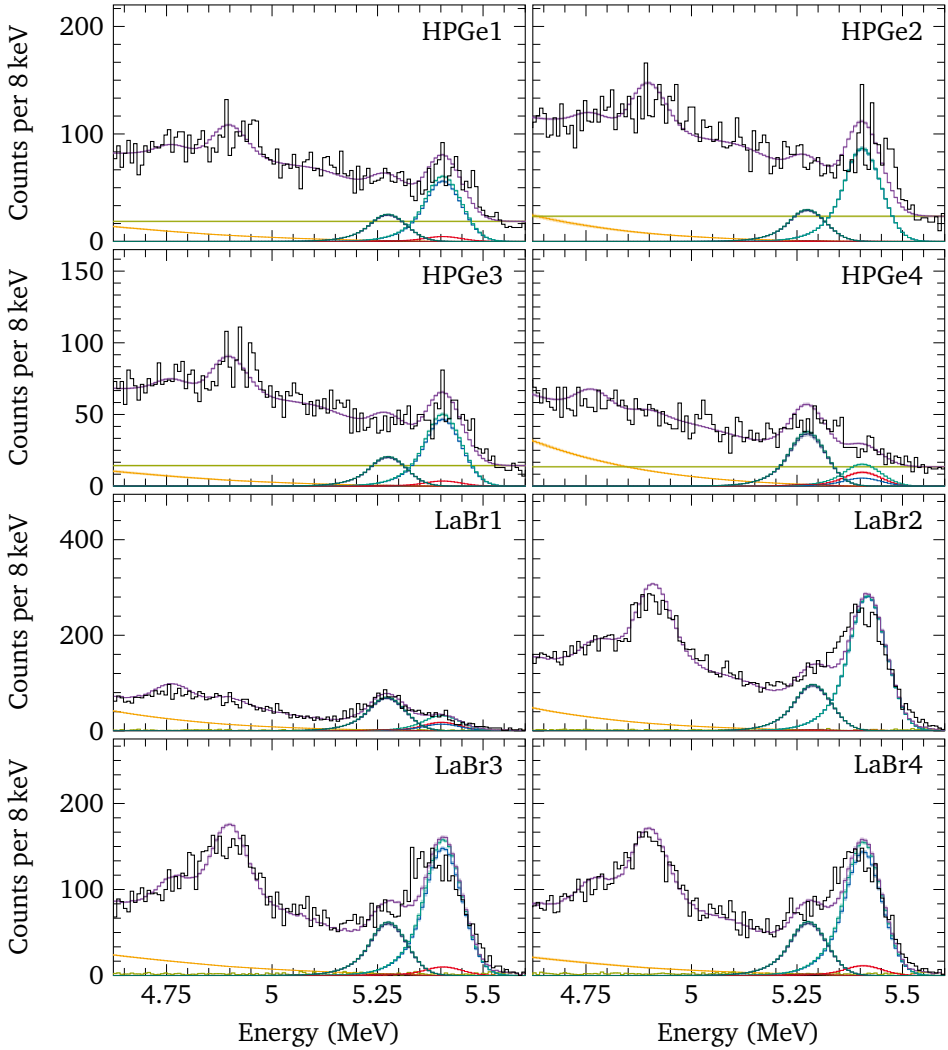

Figure 1.25: Fit of average decay branches of ^{150}Nd for $E_{\text{beam}} = 5.4\,\text{MeV}$

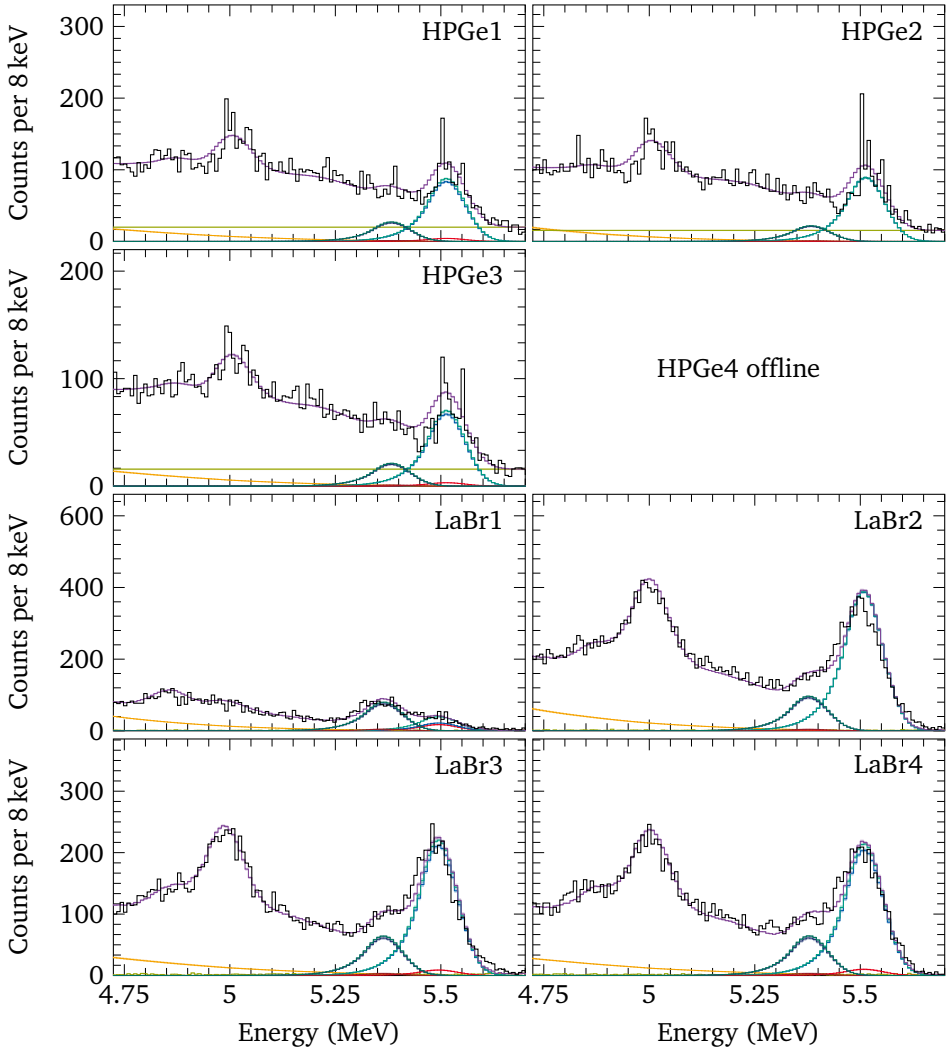

Figure 1.26: Fit of average decay branches of ^{150}Nd for $E_{\text{beam}} = 5.5\,\text{MeV}$

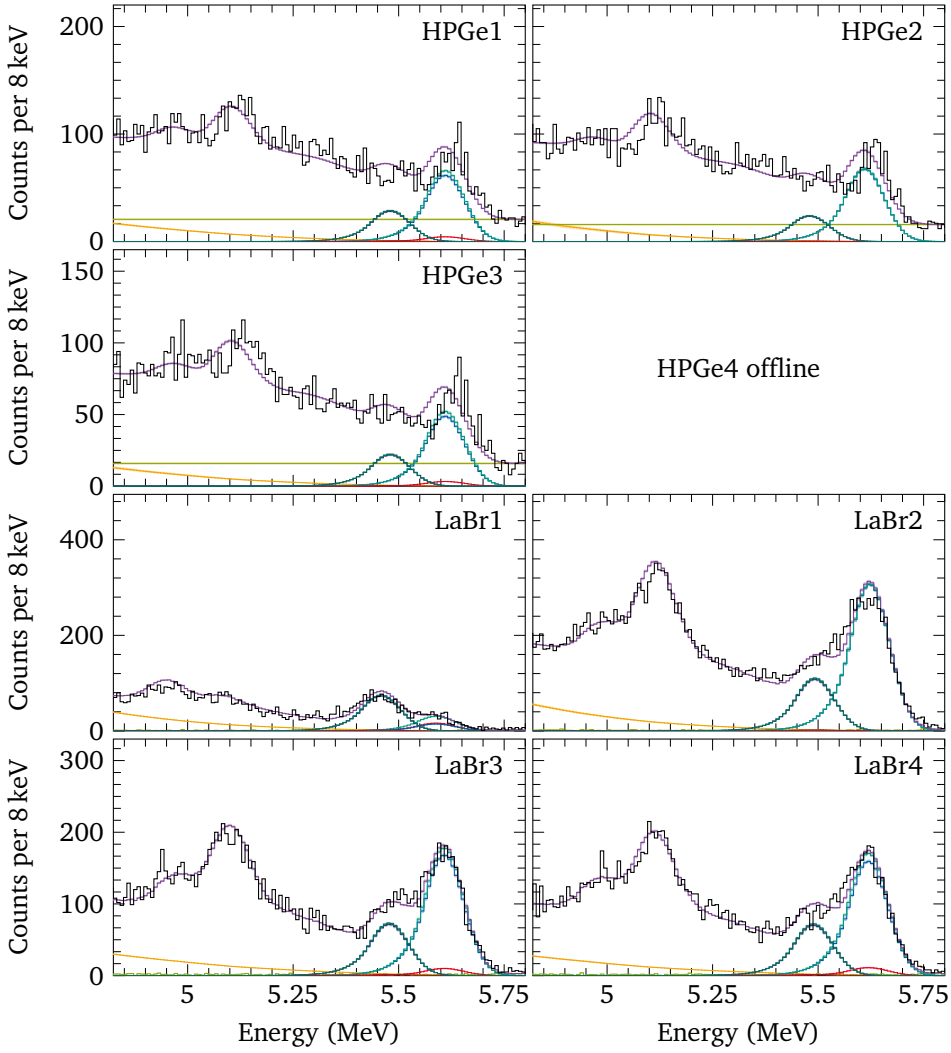

Figure 1.27: Fit of average decay branches of ^{150}Nd for $E_{\text{beam}} = 5.6\,\text{MeV}$

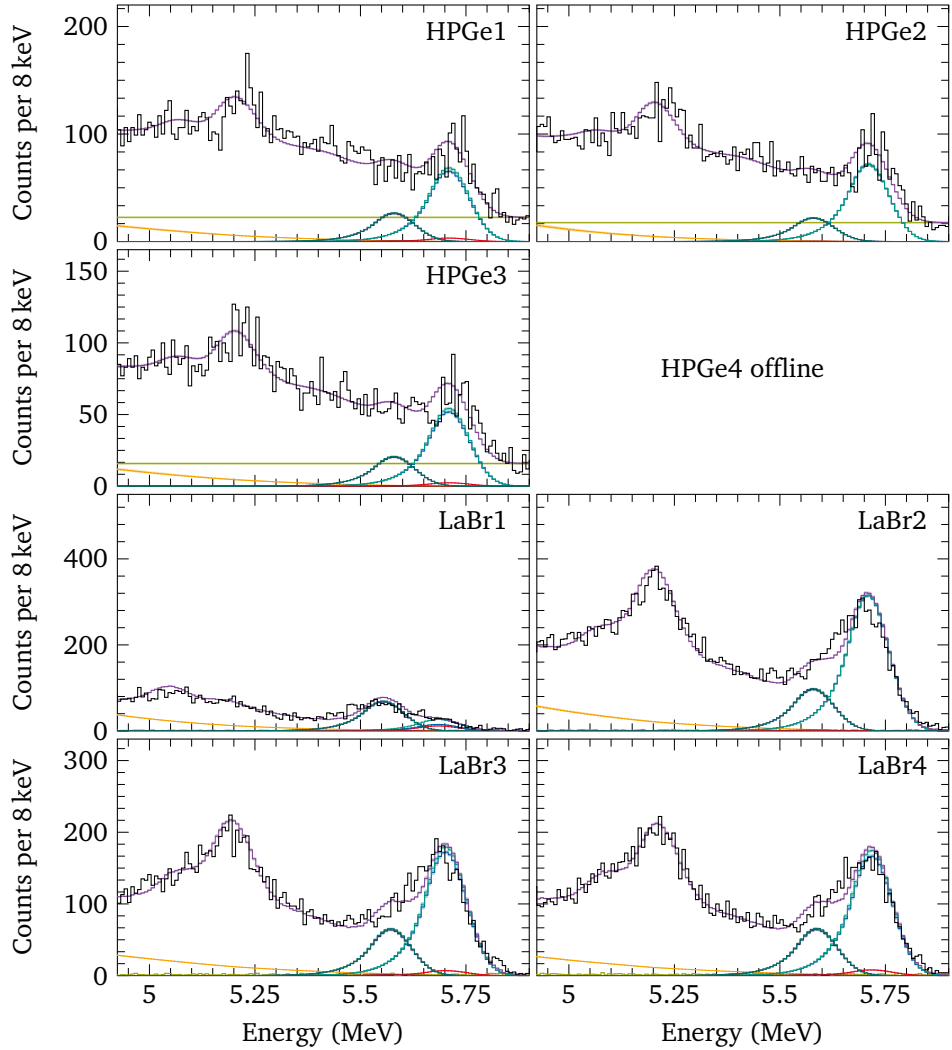

Figure 1.28: Fit of average decay branches of ^{150}Nd for $E_{\text{beam}} = 5.7\,\text{MeV}$

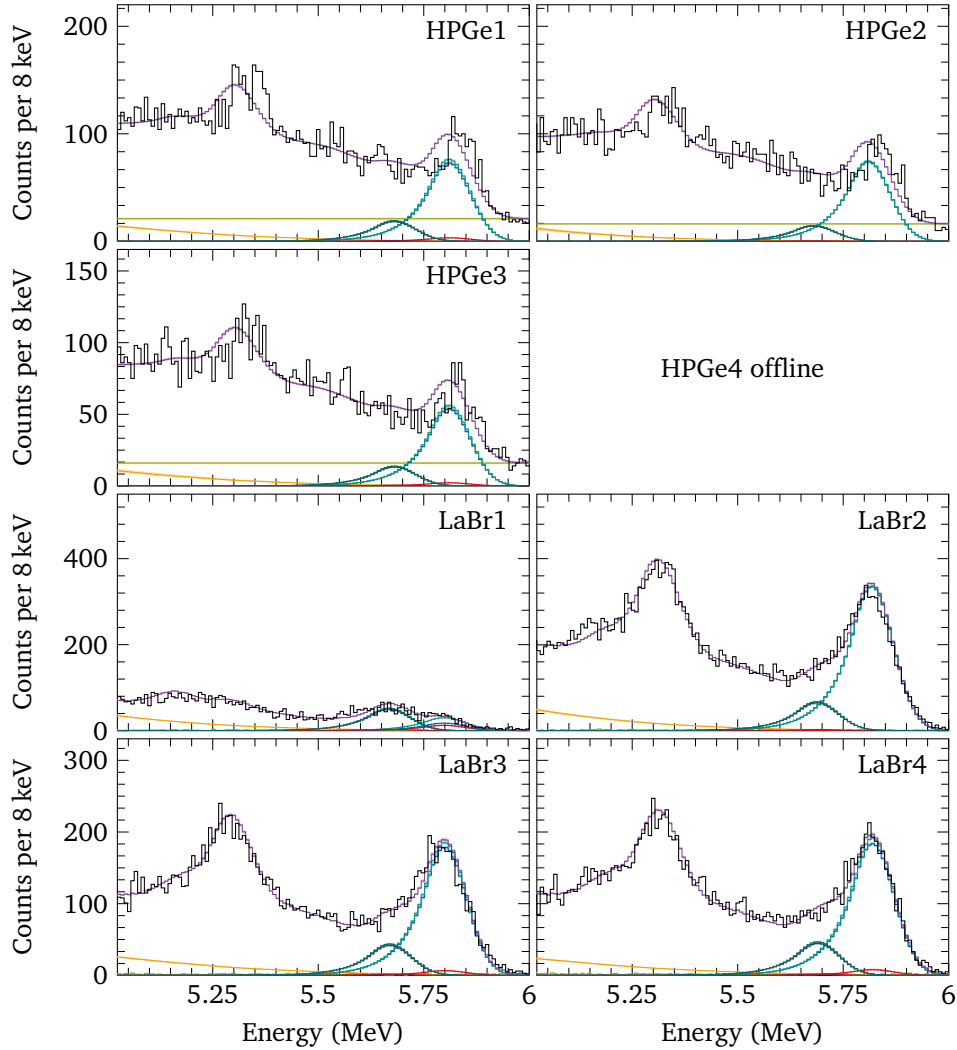

Figure 1.29: Fit of average decay branches of ^{150}Nd for $E_{\text{beam}} = 5.8\,\text{MeV}$

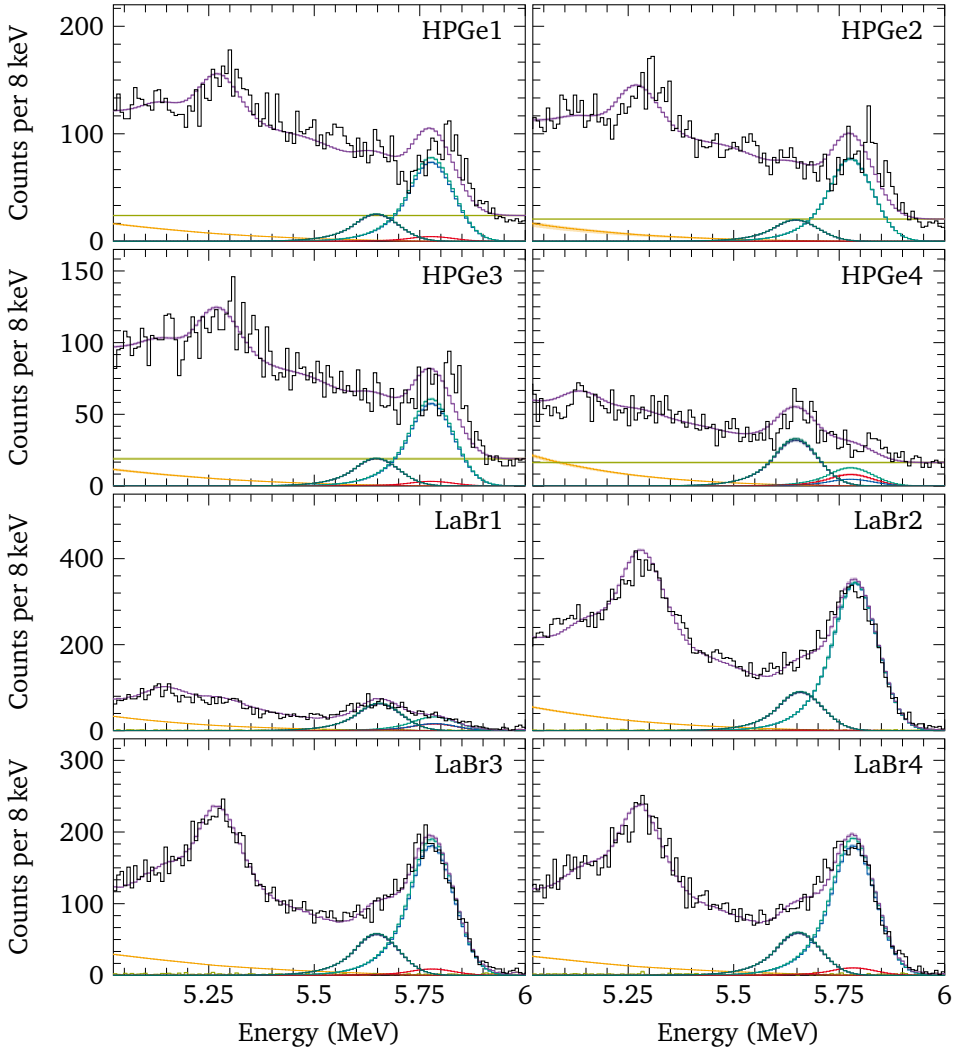

Figure 1.30: Fit of average decay branches of ^{150}Nd for $E_{\text{beam}} = 5.8\,\text{MeV}$

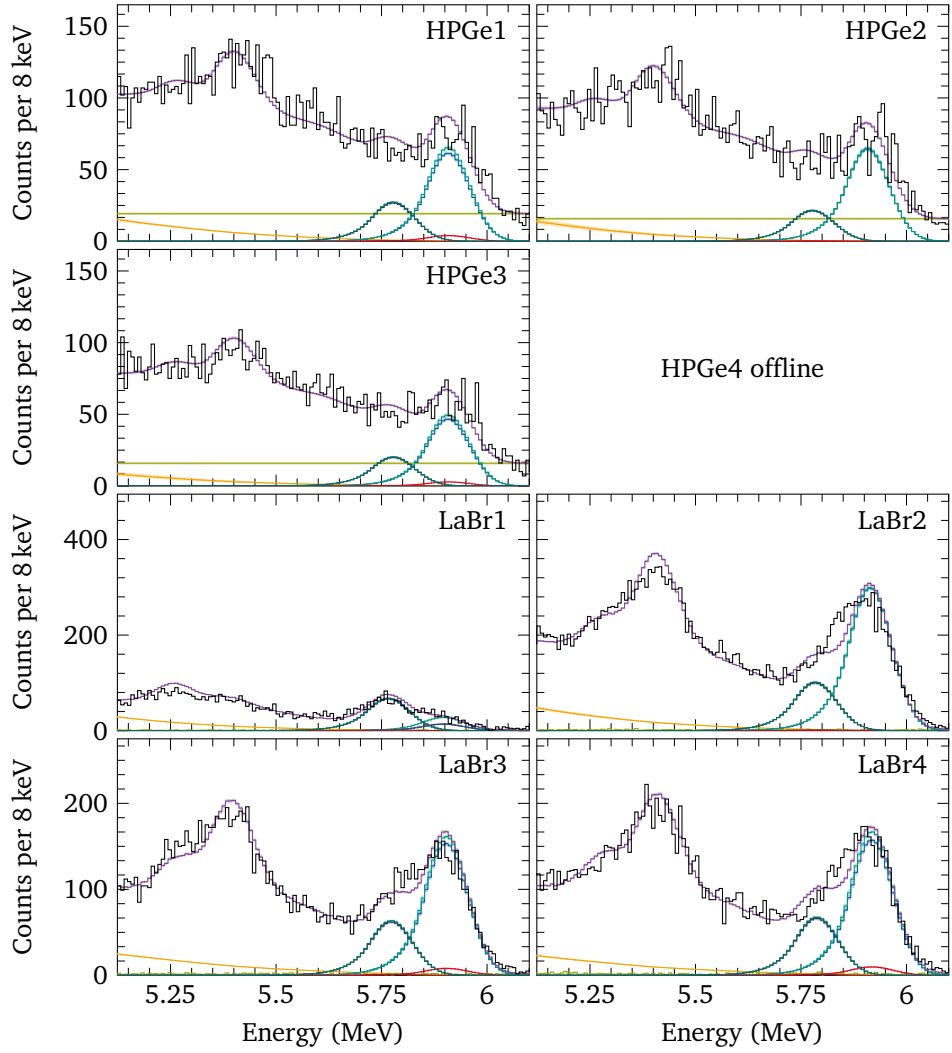

Figure 1.31: Fit of average decay branches of ^{150}Nd for $E_{\text{beam}} = 5.9\,\text{MeV}$

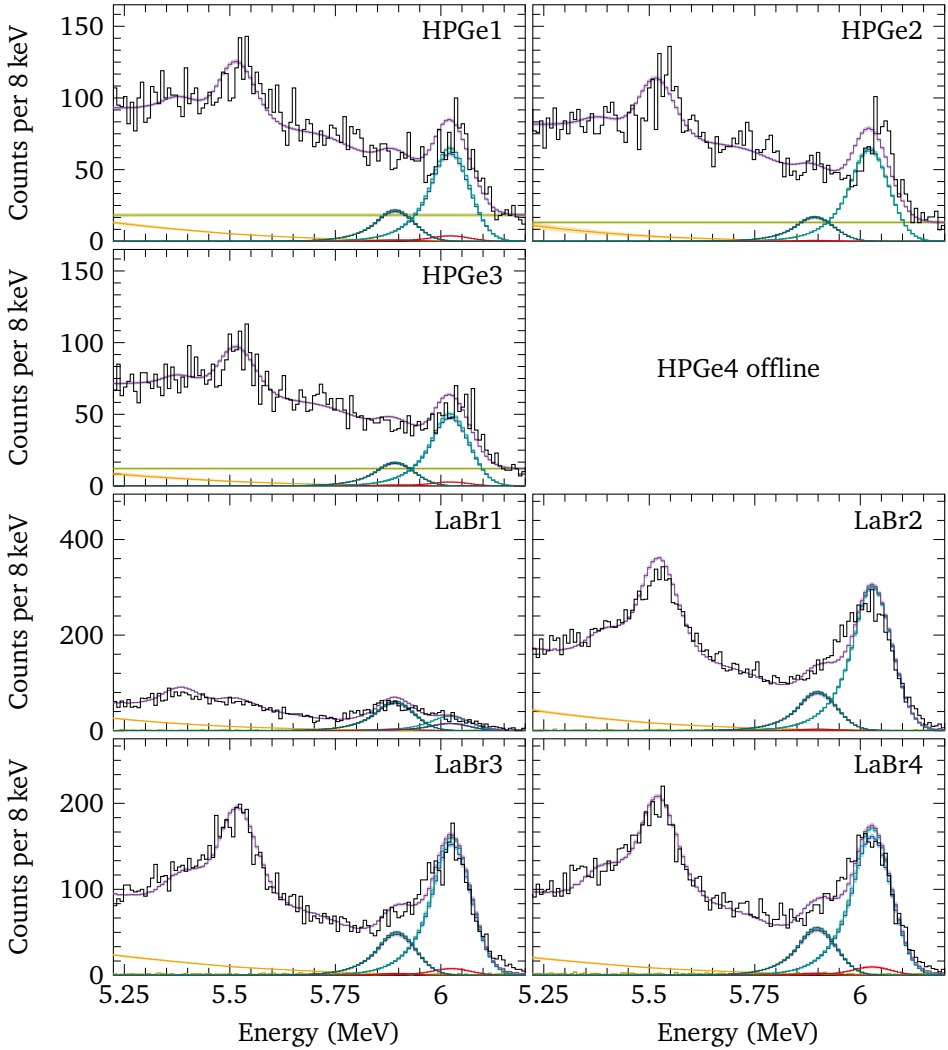

Figure 1.32: Fit of average decay branches of ^{150}Nd for $E_{\text{beam}} = 6.0\,\text{MeV}$

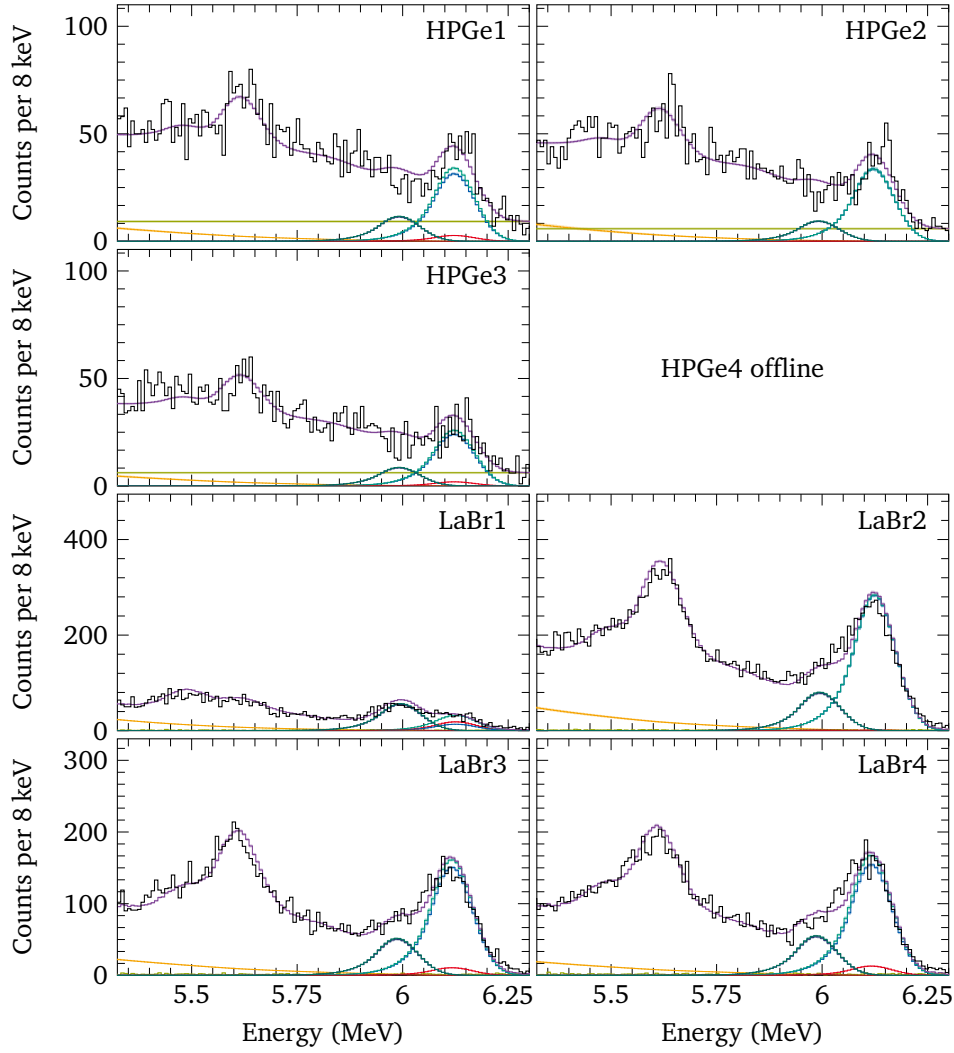

Figure 1.33: Fit of average decay branches of ^{150}Nd for $E_{\text{beam}} = 6.1\,\text{MeV}$

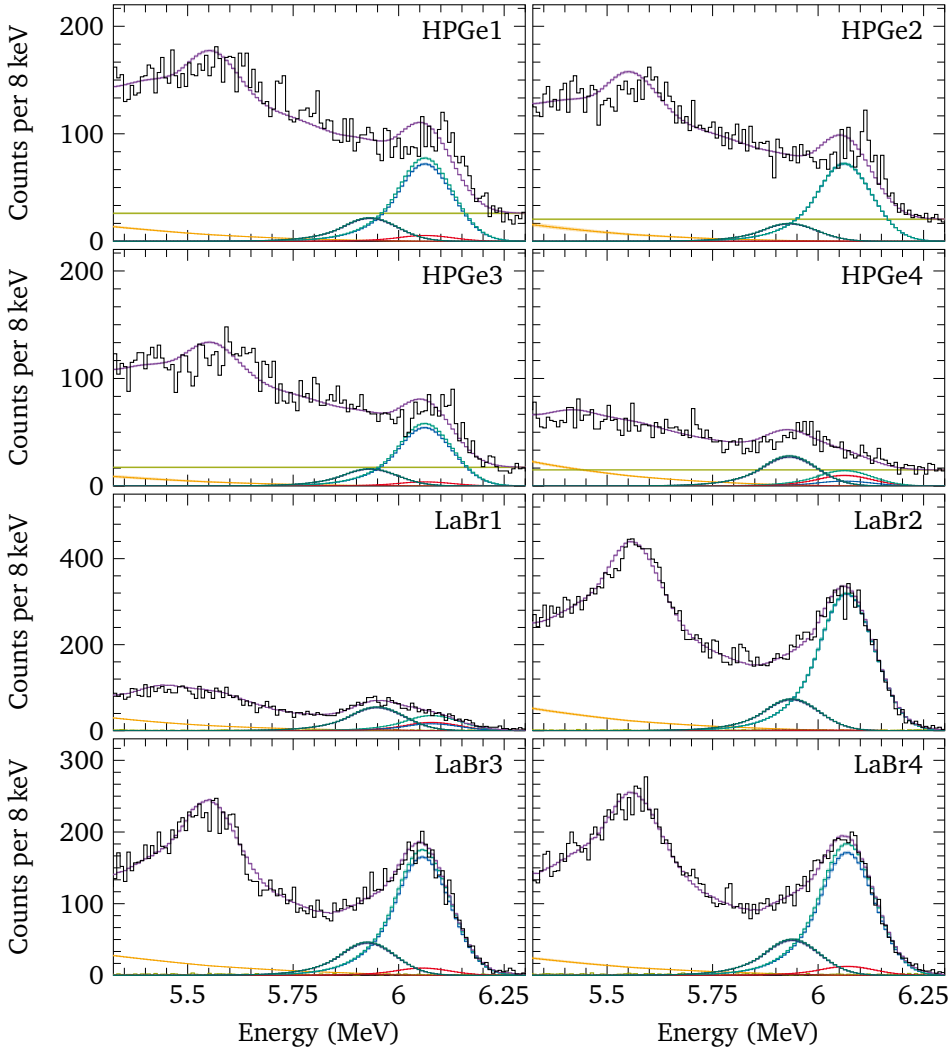

Figure 1.34: Fit of average decay branches of ^{150}Nd for $E_{\text{beam}} = 6.1$ MeV

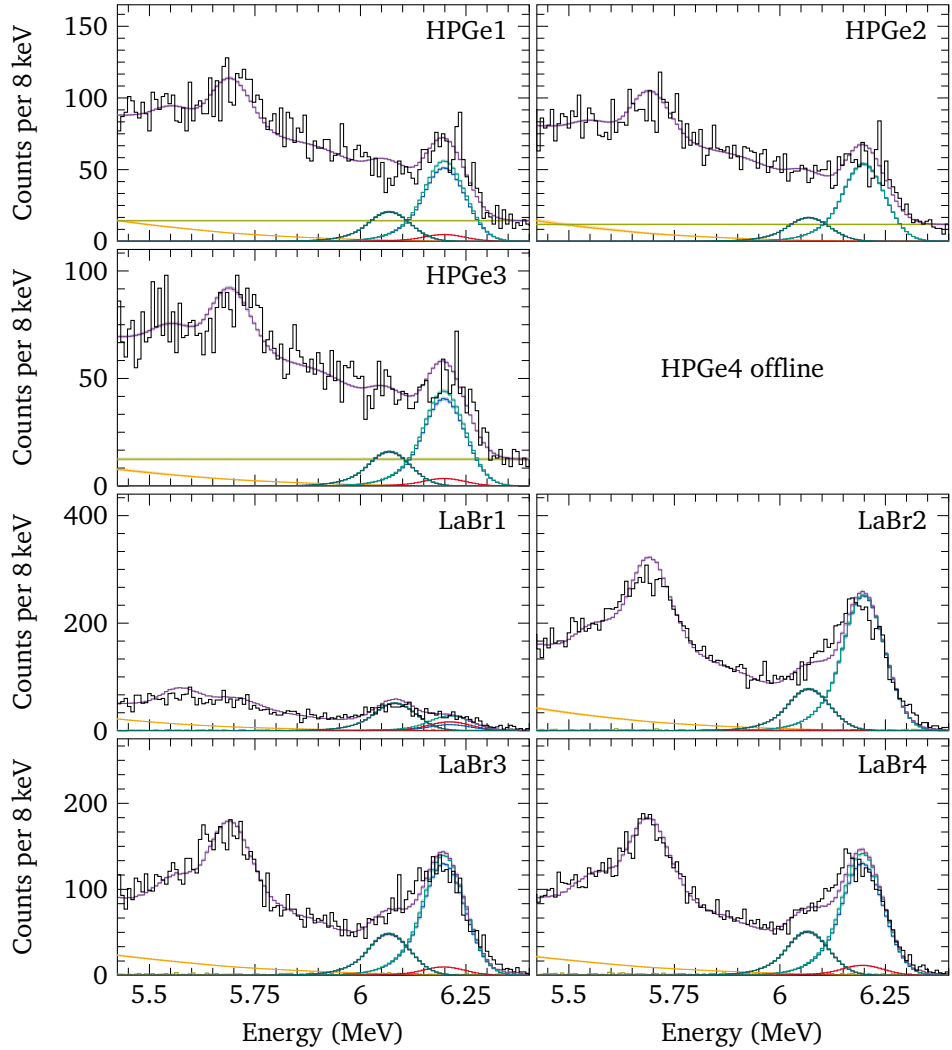

Figure 1.35: Fit of average decay branches of ^{150}Nd for $E_{\text{beam}} = 6.2\,\text{MeV}$

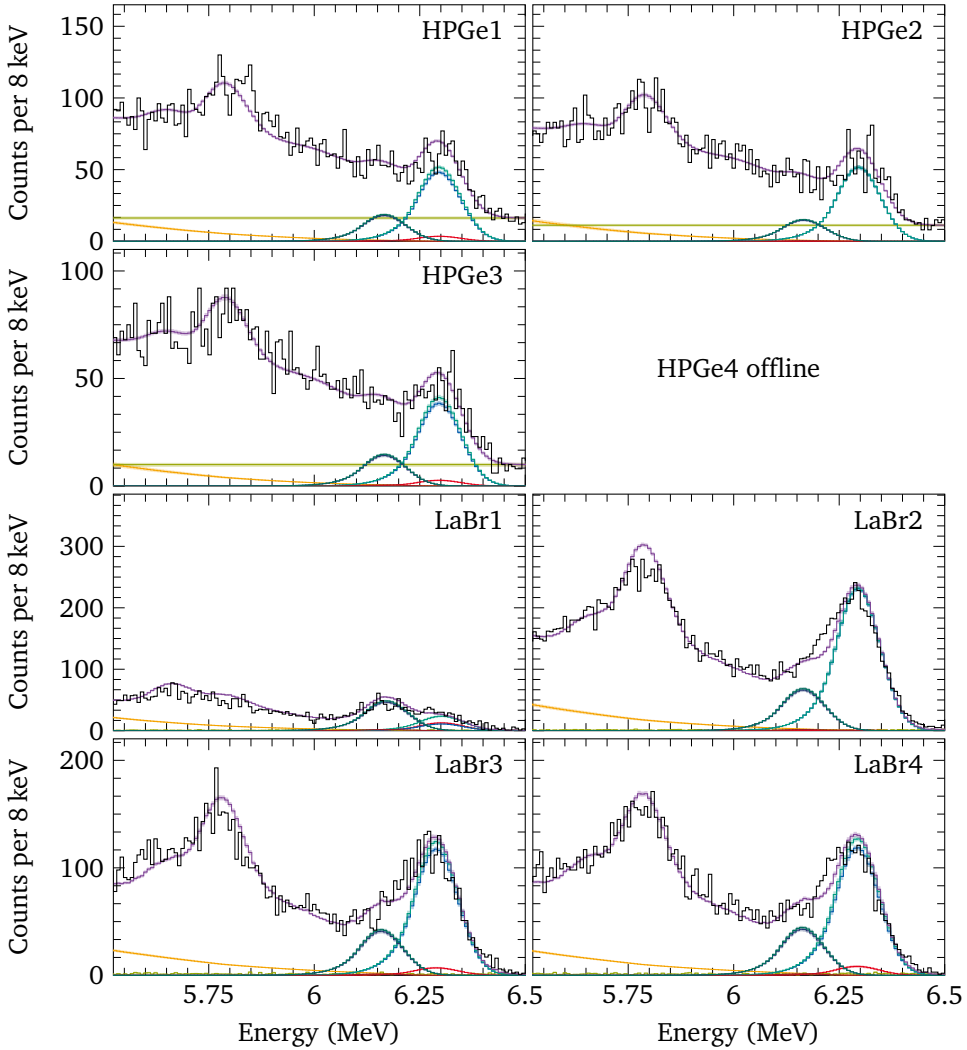

Figure 1.36: Fit of average decay branches of ^{150}Nd for $E_{\text{beam}} = 6.3\,\text{MeV}$

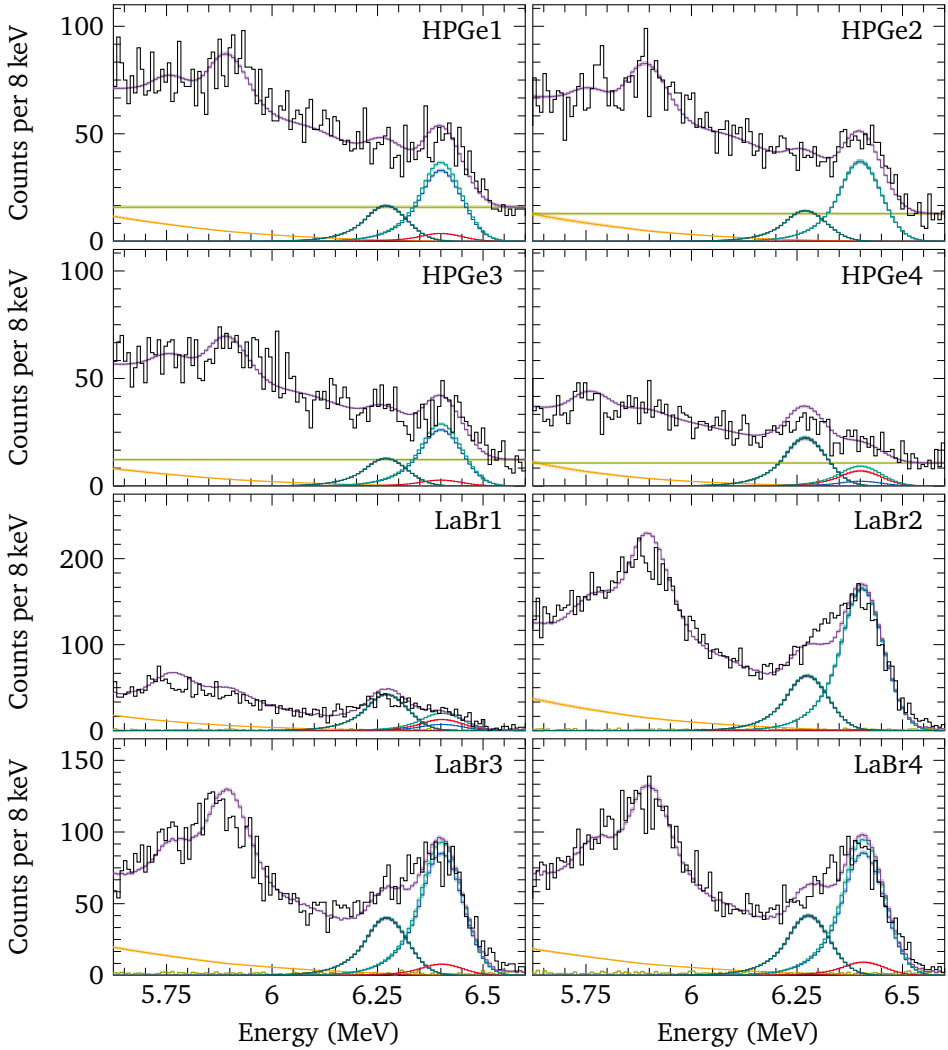

Figure 1.37: Fit of average decay branches of ^{150}Nd for $E_{\text{beam}} = 6.4\,\text{MeV}$

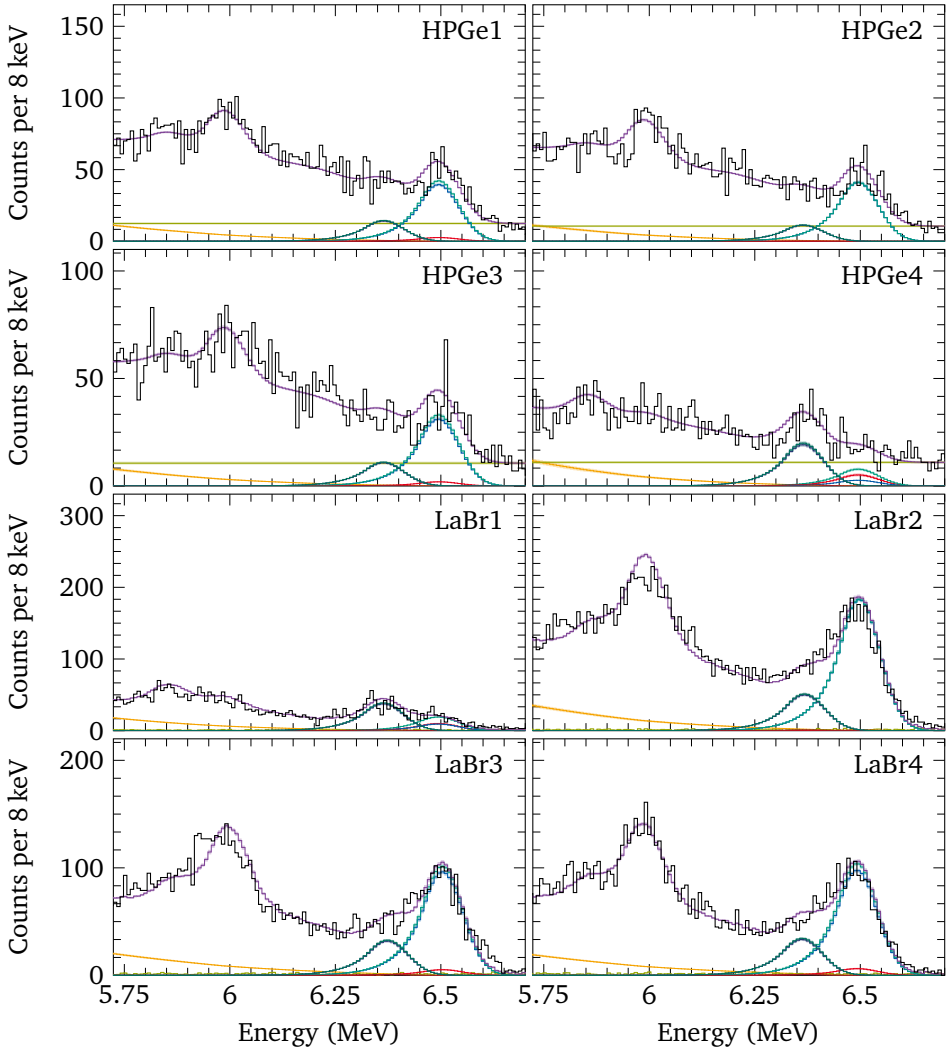

Figure 1.38: Fit of average decay branches of ^{150}Nd for $E_{\text{beam}} = 6.5\,\text{MeV}$

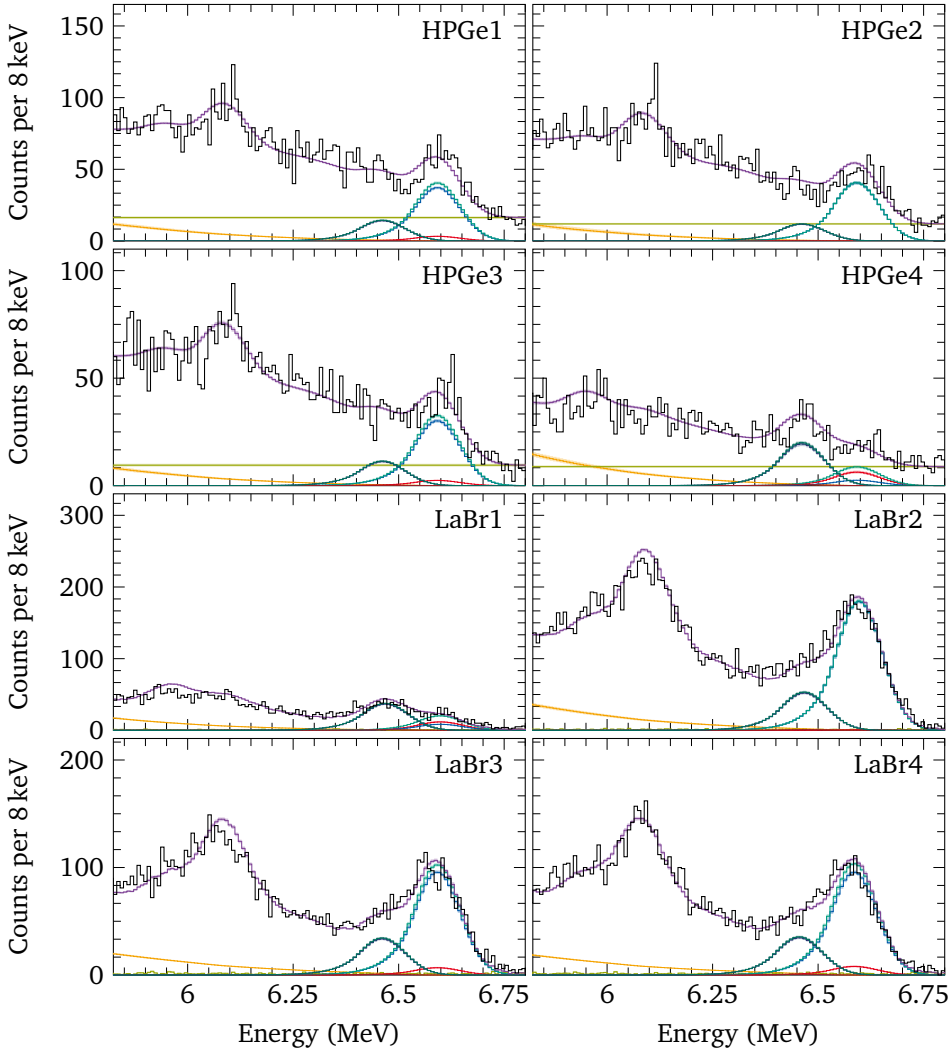

Figure 1.39: Fit of average decay branches of ^{150}Nd for $E_{\text{beam}} = 6.6\,\text{MeV}$

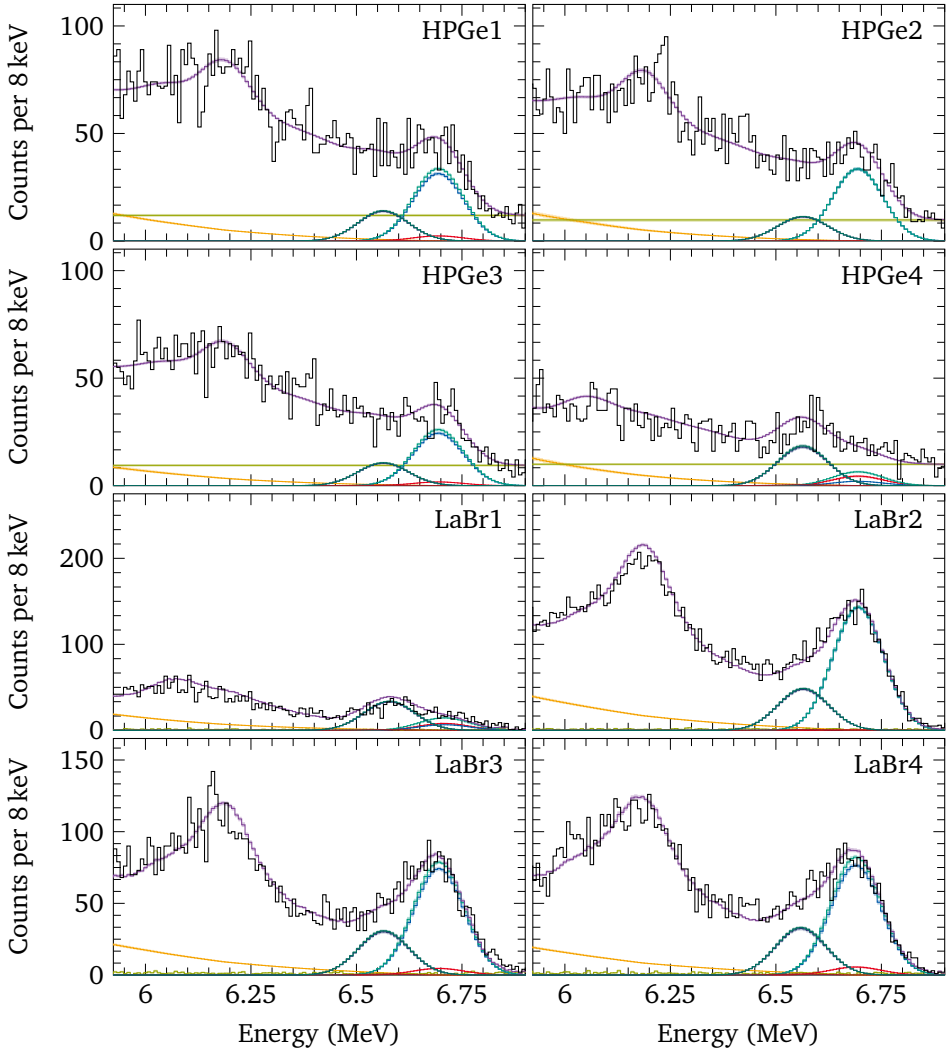

Figure 1.40: Fit of average decay branches of ^{150}Nd for $E_{\text{beam}} = 6.7\,\text{MeV}$

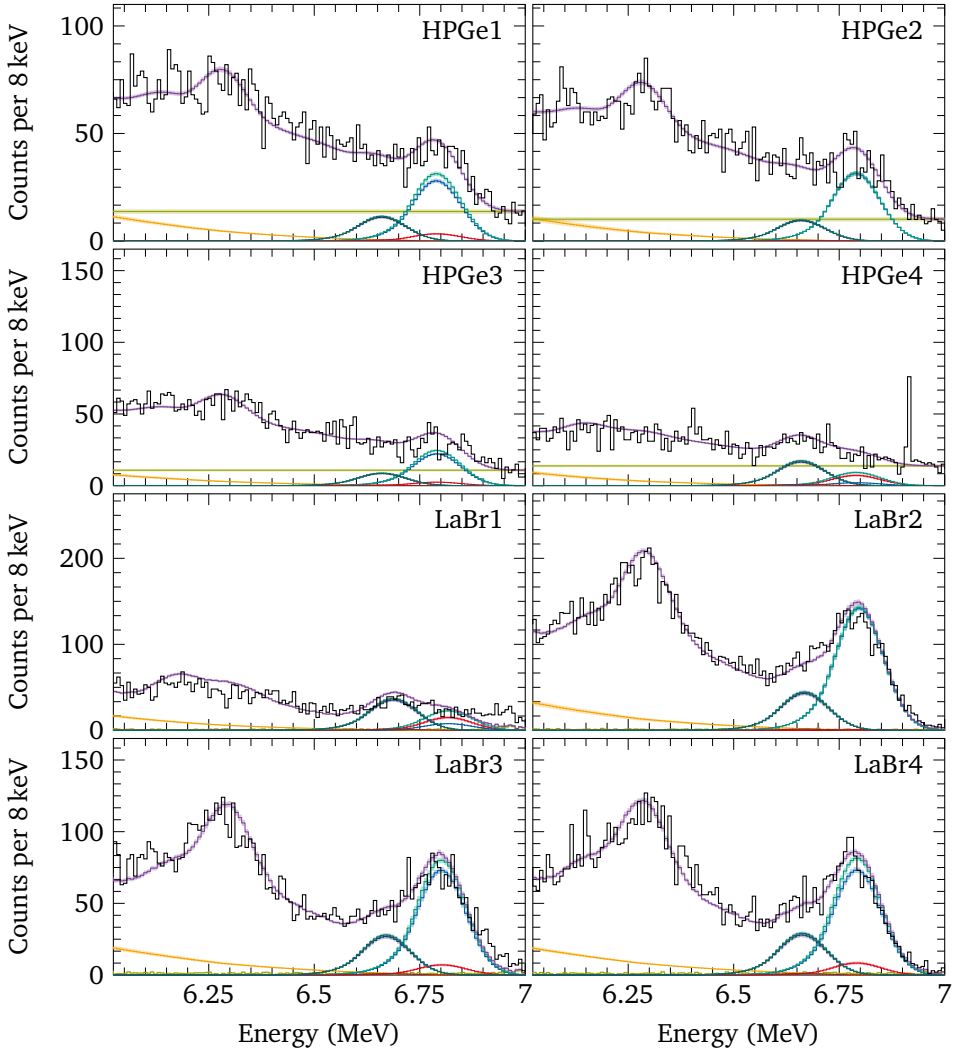

Figure 1.41: Fit of average decay branches of ^{150}Nd for $E_{\text{beam}} = 6.8\,\text{MeV}$

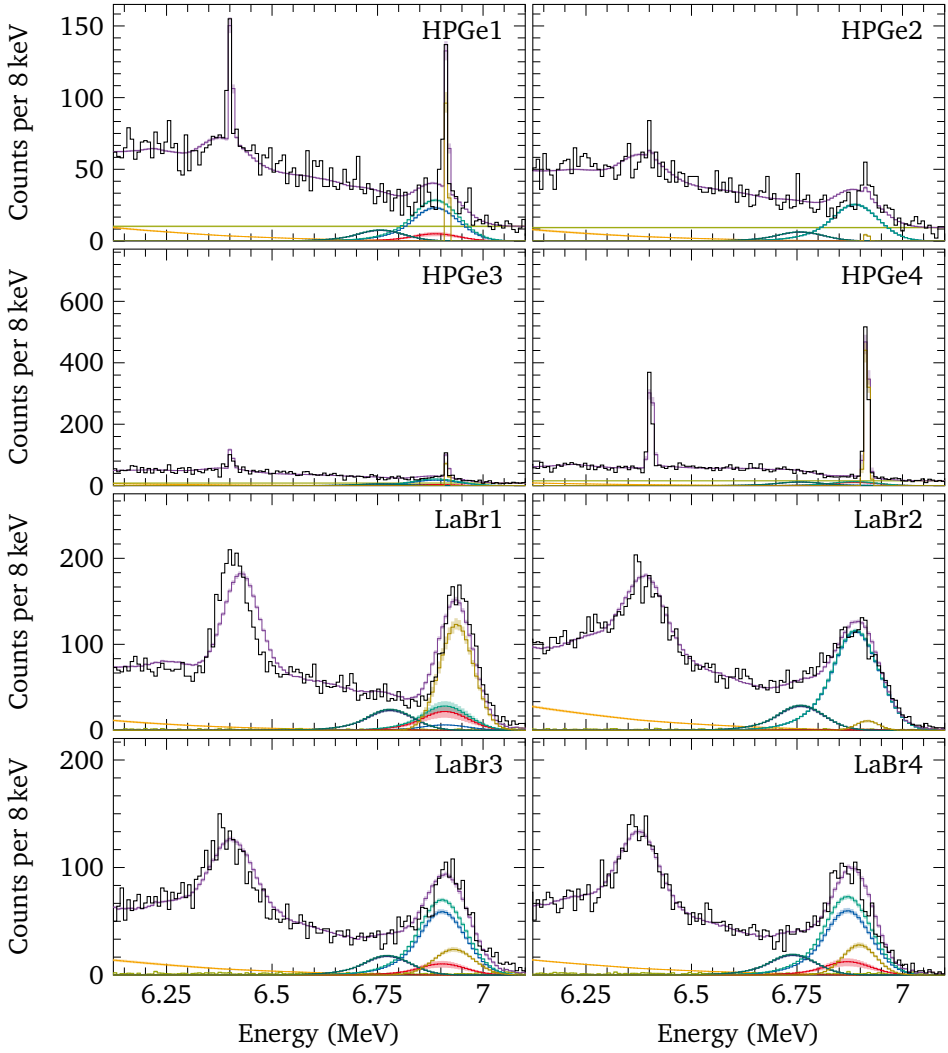

Figure 1.42: Fit of average decay branches of ^{150}Nd for $E_{\text{beam}} = 6.9\,\text{MeV}$

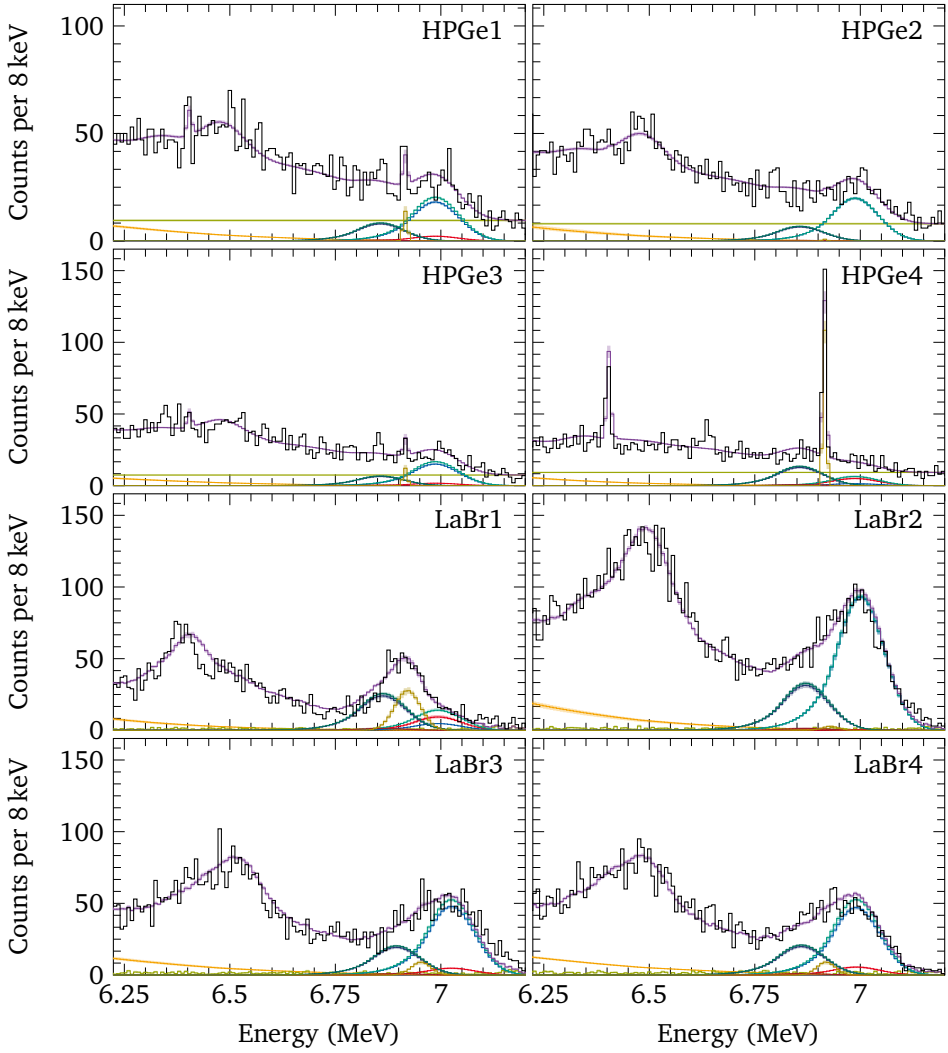

Figure 1.43: Fit of average decay branches of ^{150}Nd for $E_{\text{beam}} = 7.0\,\text{MeV}$

2 HPGe spectra of ^{150}Nd for DHIPS and HIγS

The figures in this section show detailed HPGe spectra for both the DHIPS and HIγS ^{150}Nd experiment. The binning is 1 keV, except for HPGe4 for runs with a bad resolution. For some beam energies, HPGe4 was missing. Each figure depicts severals HIγS runs in different colors. The spectral distribution of the corresponding incident photon beam is indicated by a dashed line with matching color. Gray vertical lines mark the energies of transitions of excited states of ^{150}Nd to the 0_1^+ and 2_1^+ state. This also includes transitions to the 2_1^+ state that were not analyzed. Further markers indicate transition energies of excited states of ^{12}C, ^{16}O, ^{27}Al and also background lines.

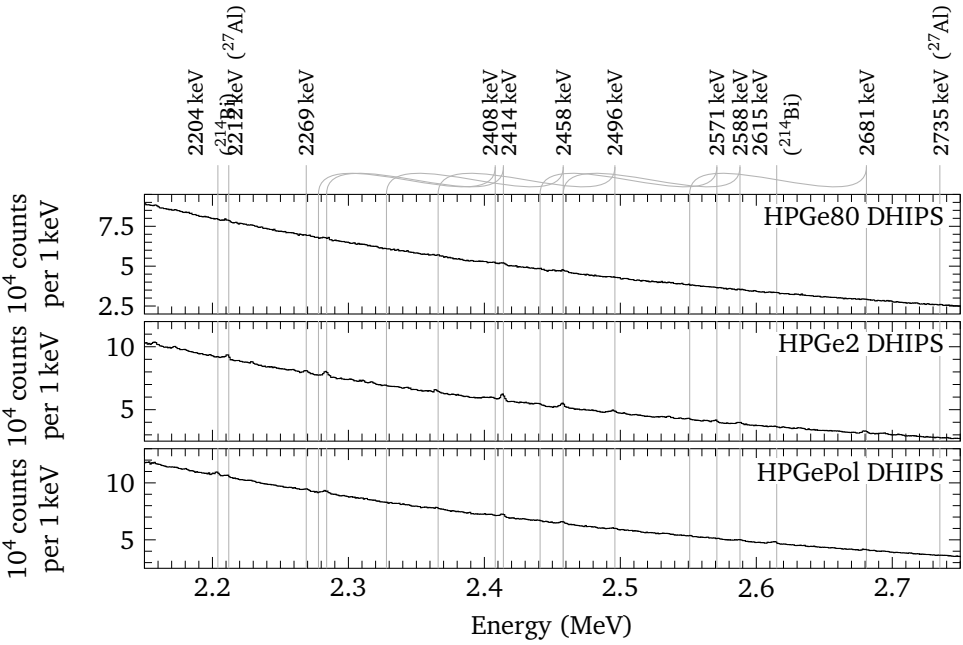

Figure 2.1: DHIPS ^{150}Nd HPGe spectra for 2.2 MeV to 2.7 MeV.

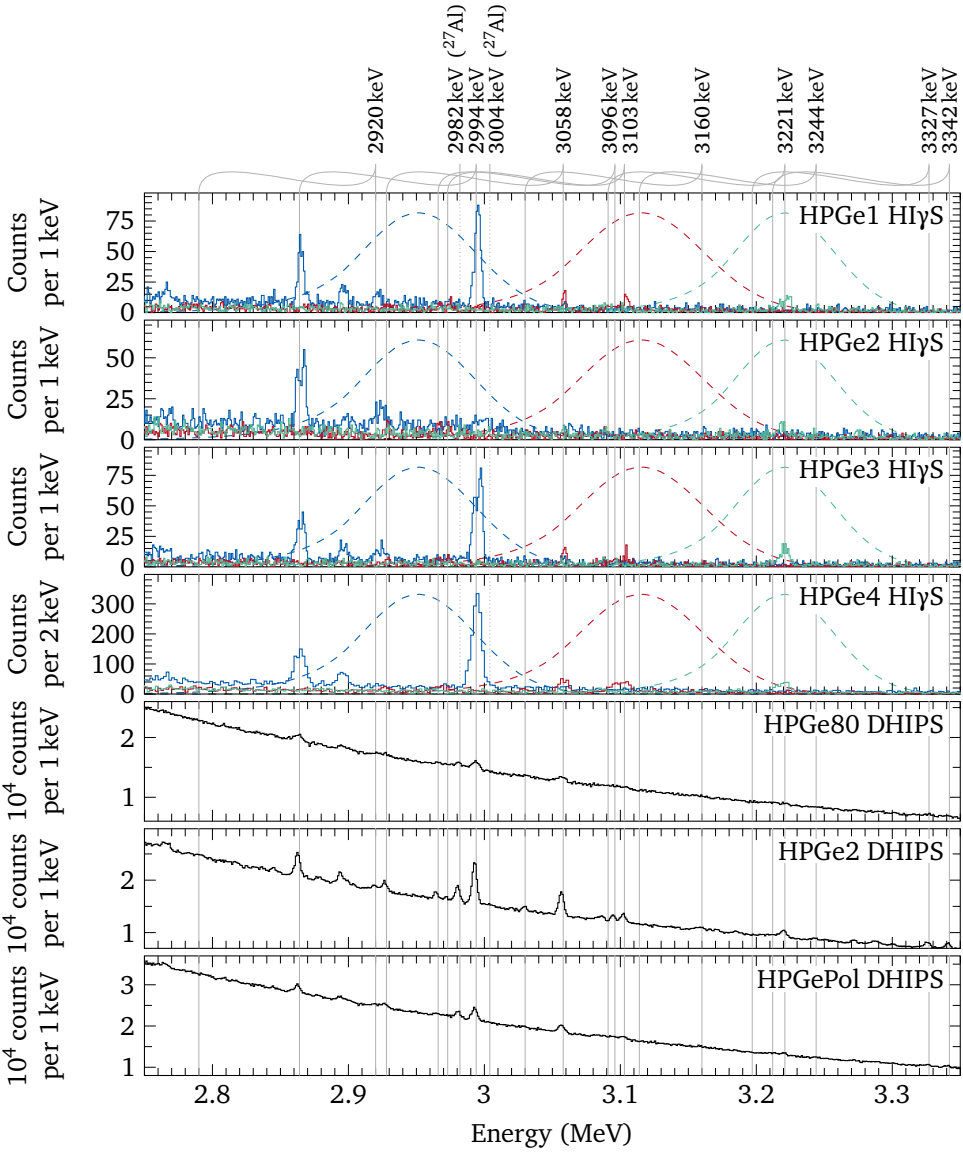

Figure 2.2: DHIPS and HIγS ^{150}Nd HPGe spectra for 2.8 MeV to 3.3 MeV.

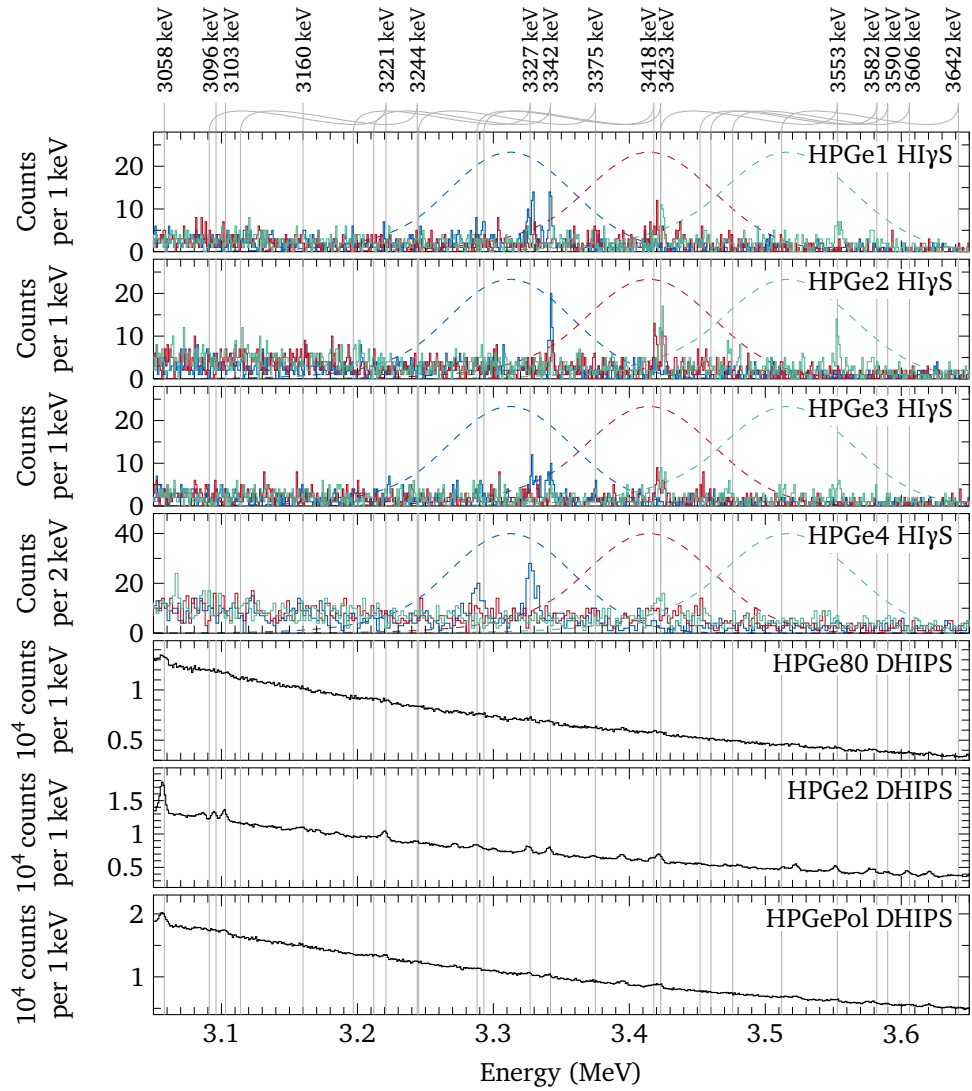

Figure 2.3: DHIPS and HIγS ^{150}Nd HPGe spectra for 3.1 MeV to 3.6 MeV.

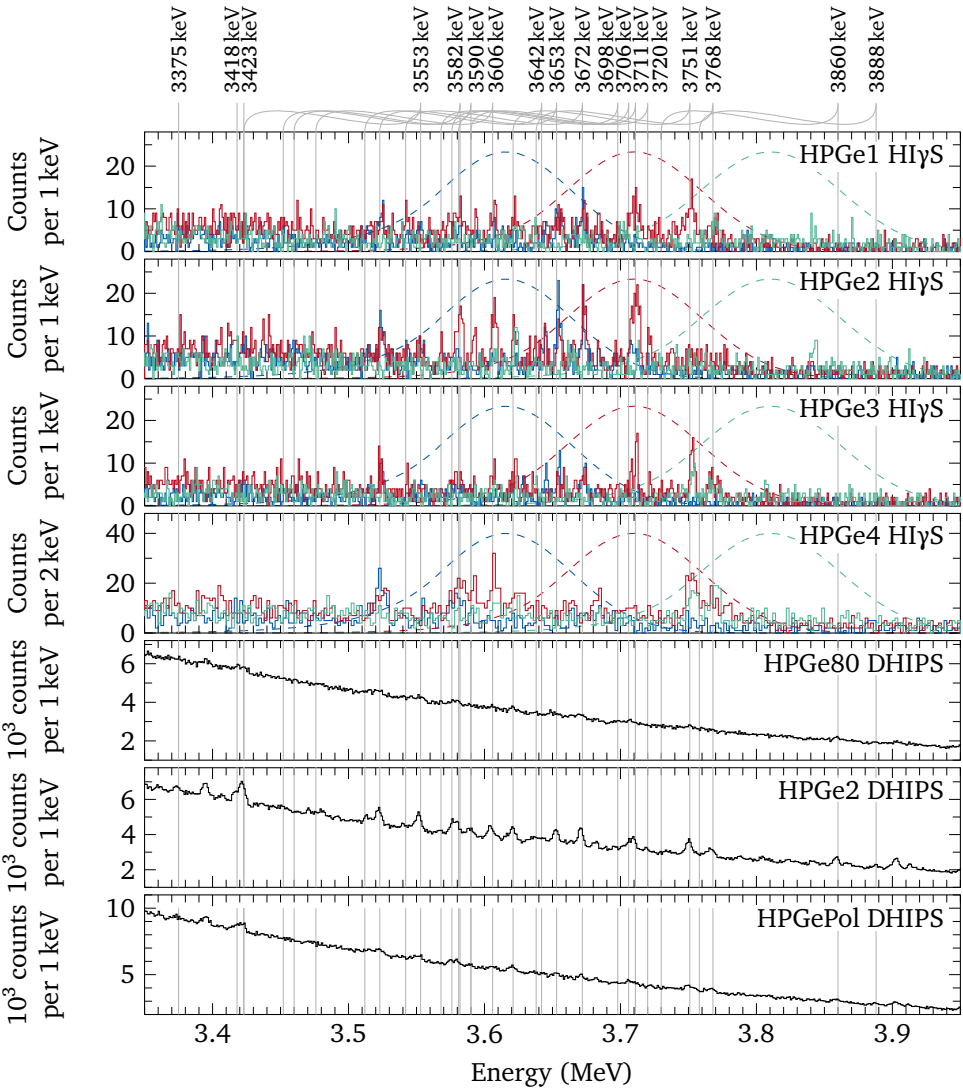

Figure 2.4: DHIPS and HIγS ^{150}Nd HPGe spectra for 3.4 MeV to 3.9 MeV.

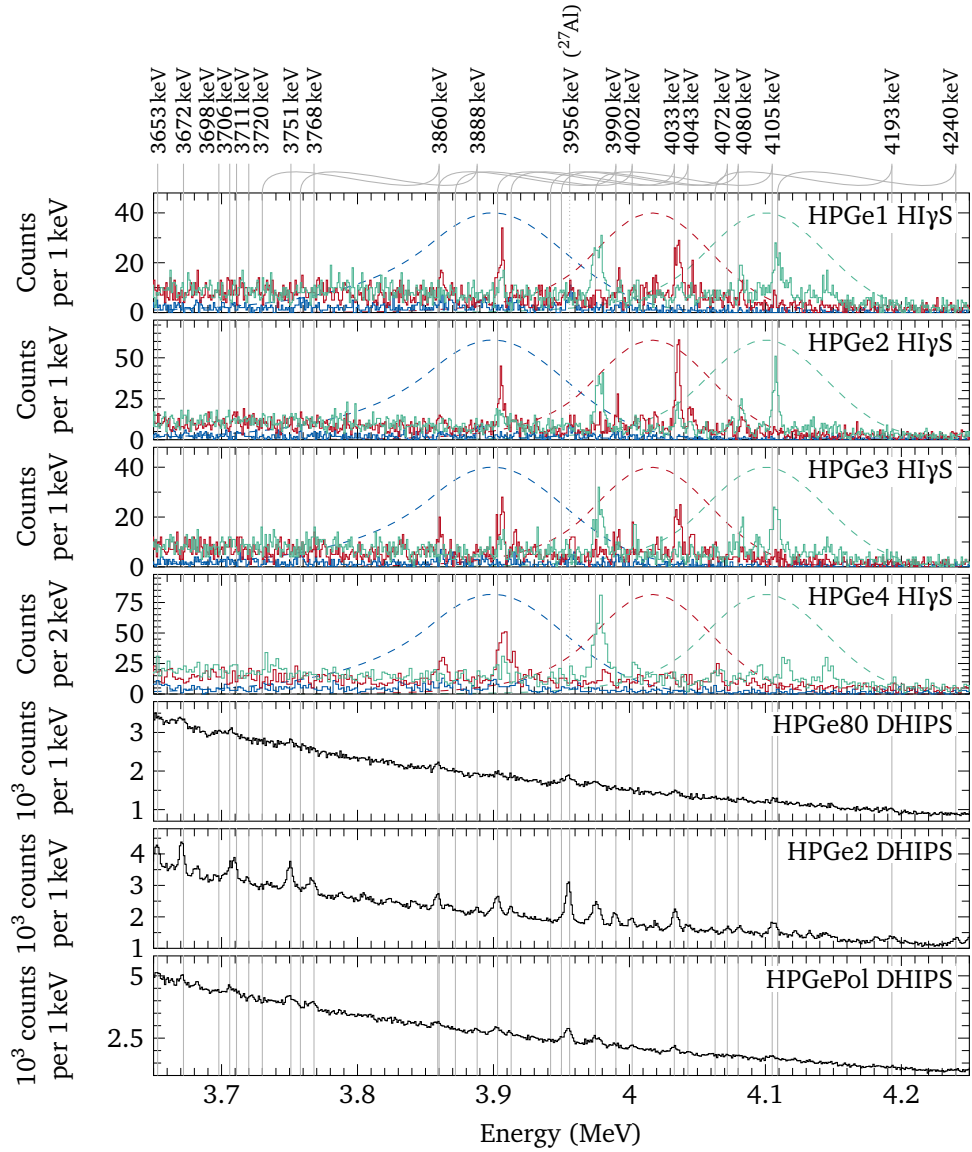

Figure 2.5: DHIPS and HIγS ^{150}Nd HPGe spectra for 3.7 MeV to 4.2 MeV.

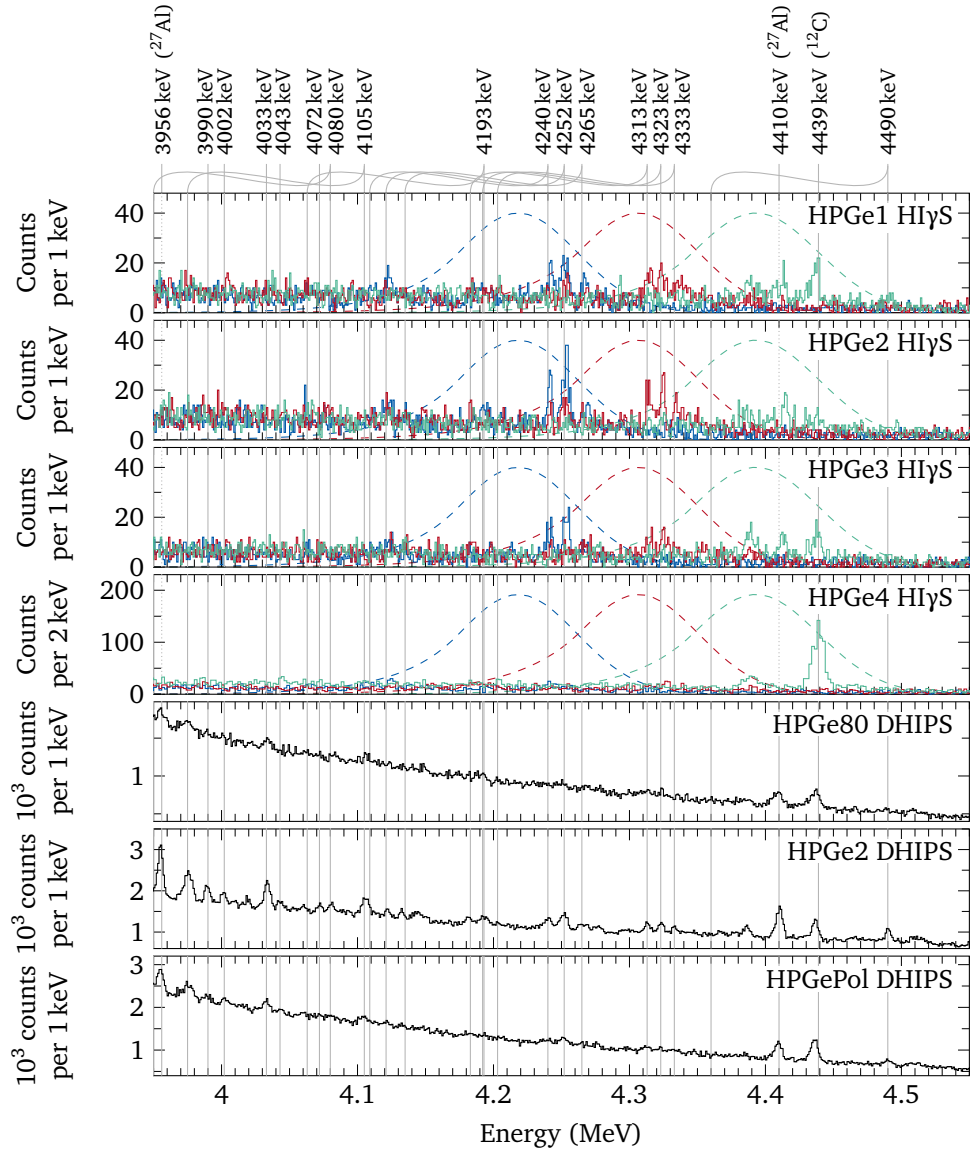

Figure 2.6: DHIPS and HIγS ^{150}Nd HPGe spectra for 4.0 MeV to 4.5 MeV.

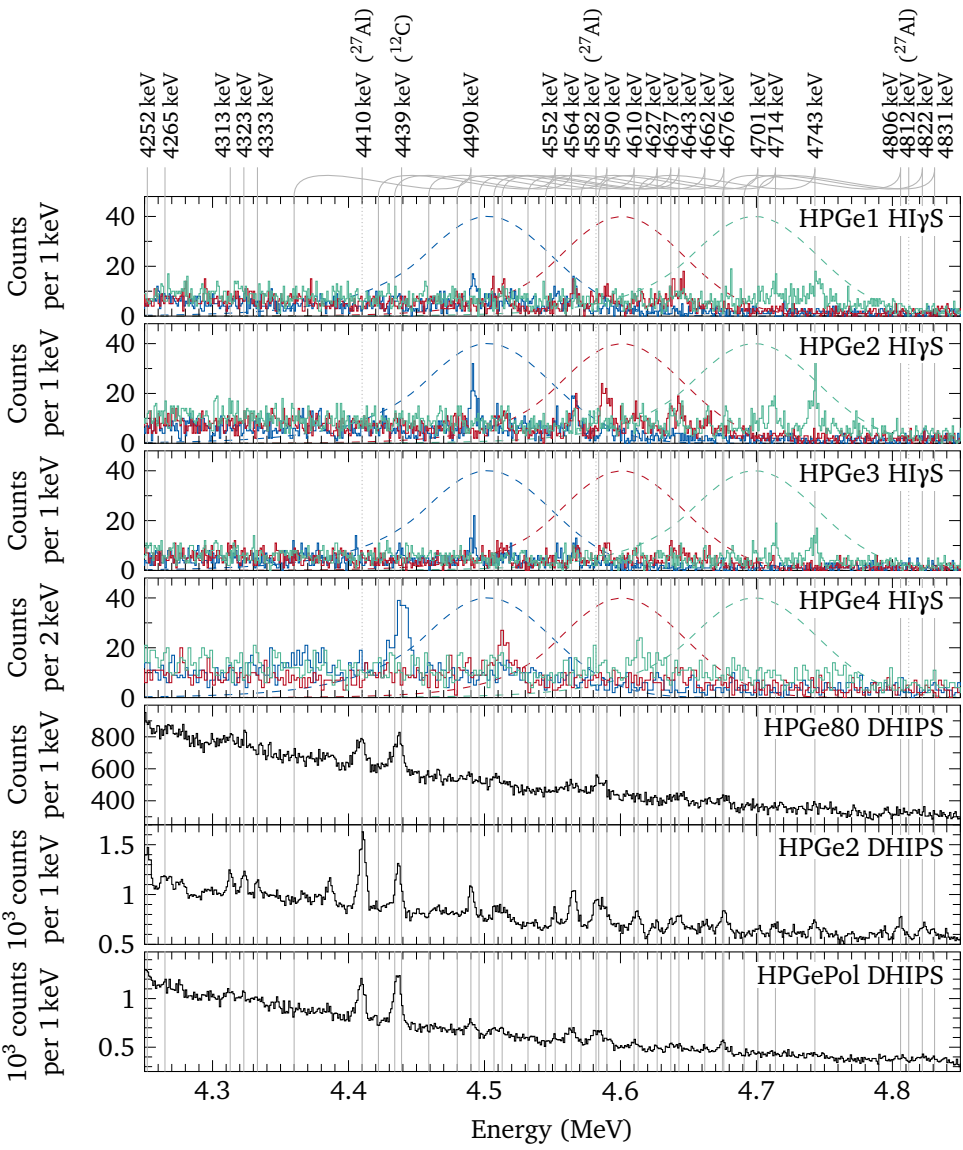

Figure 2.7: DHIPS and HIγS ^{150}Nd HPGe spectra for 4.3 MeV to 4.8 MeV.

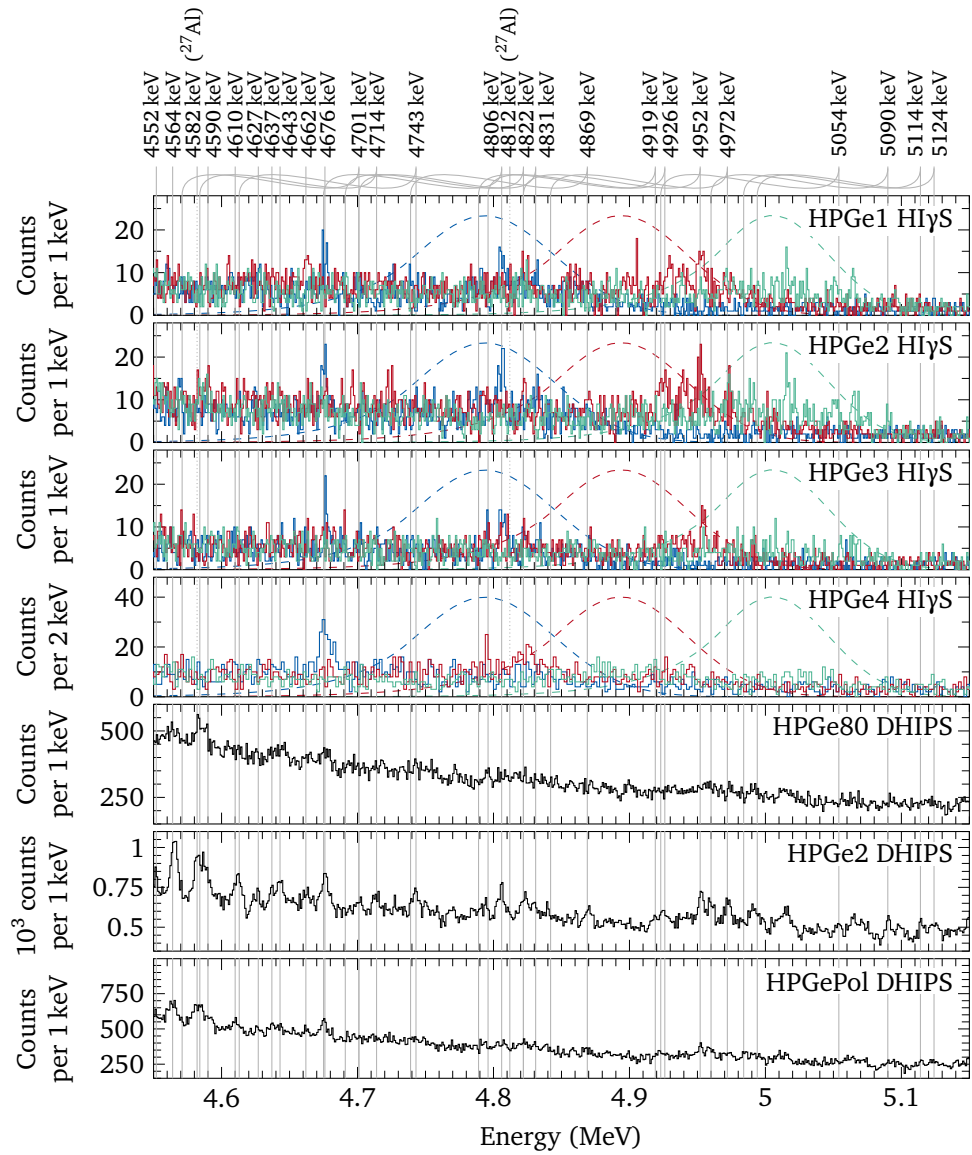

Figure 2.8: DHIPS and HIγS ^{150}Nd HPGe spectra for 4.6 MeV to 5.1 MeV.

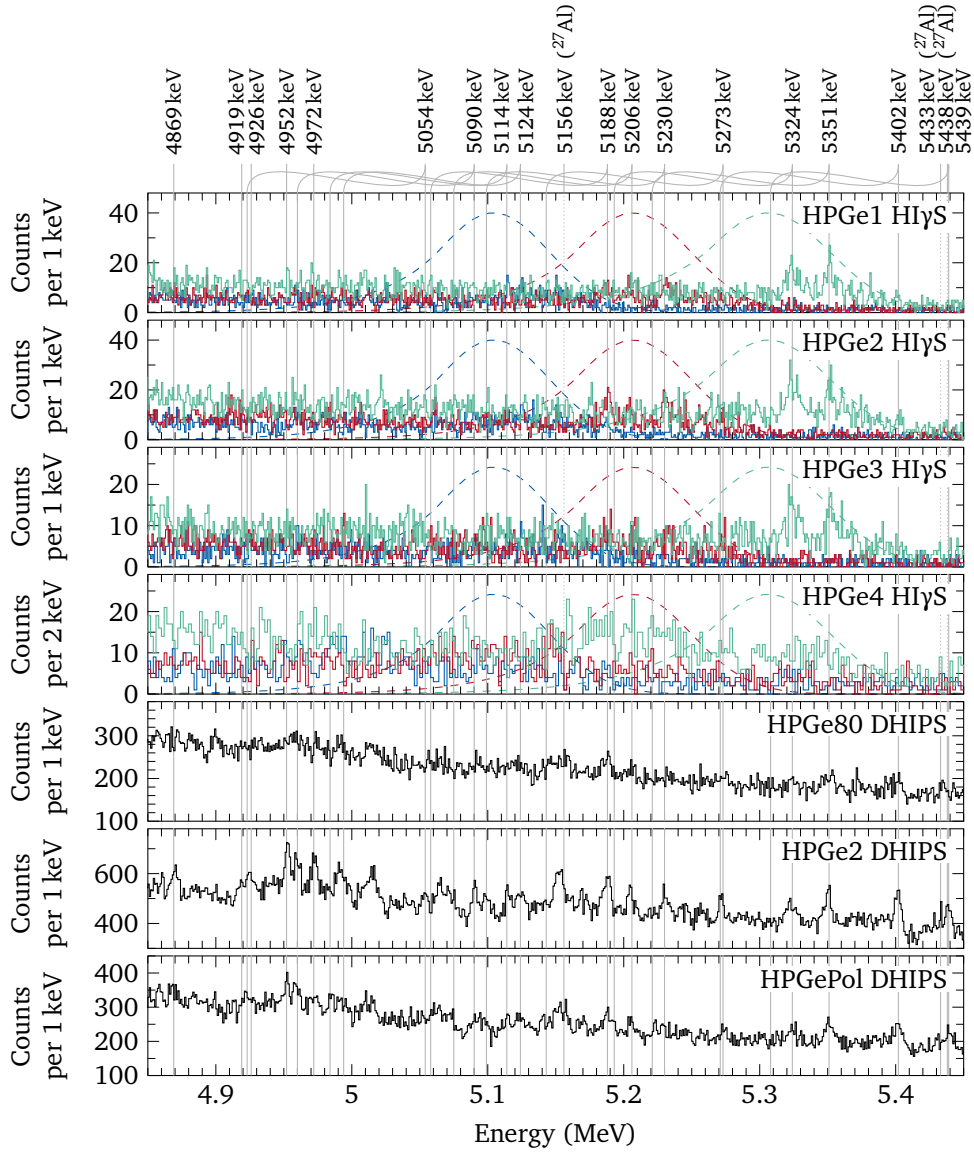

Figure 2.9: DHIPS and HIγS ^{150}Nd HPGe spectra for 4.9 MeV to 5.4 MeV.

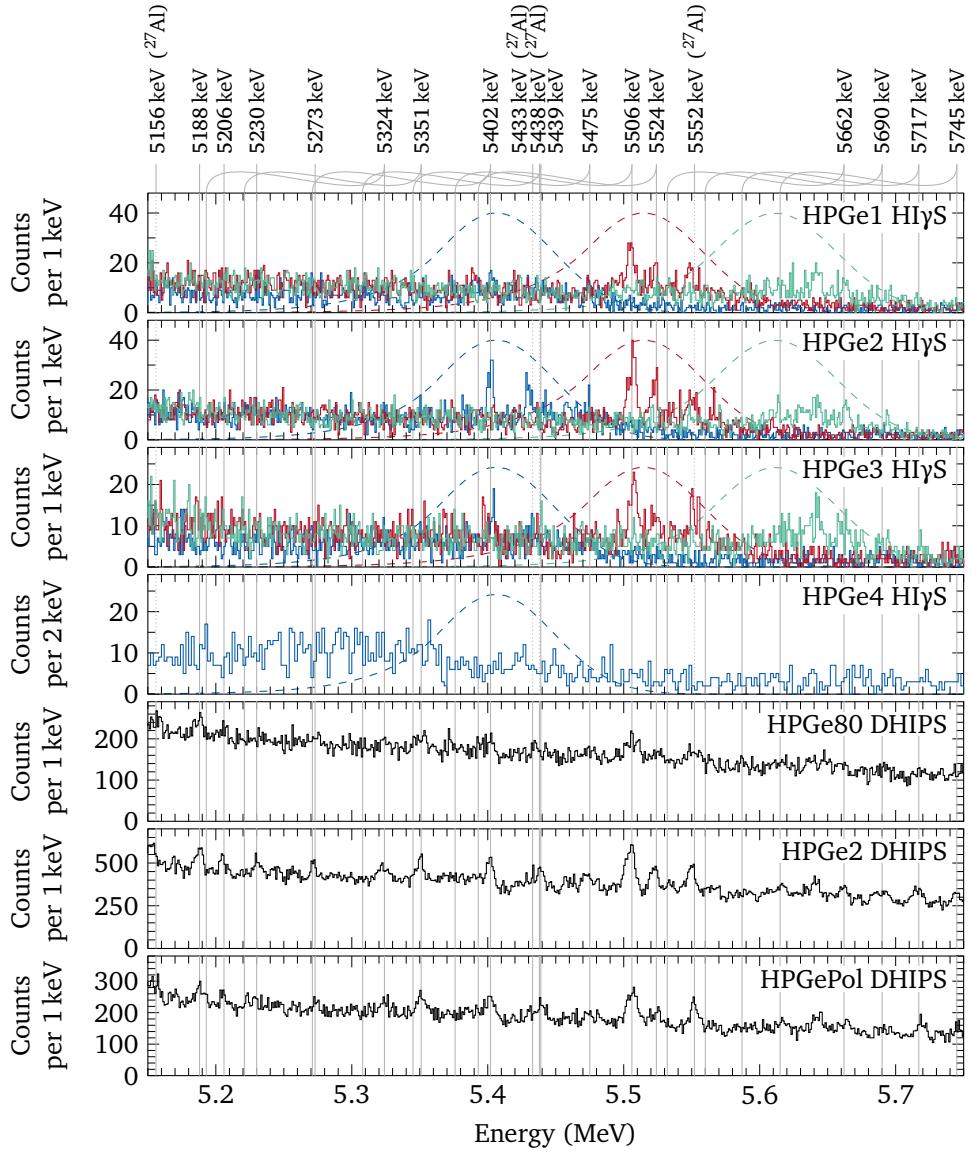

Figure 2.10: DHIPS and HIγS ^{150}Nd HPGe spectra for 5.2 MeV to 5.7 MeV.

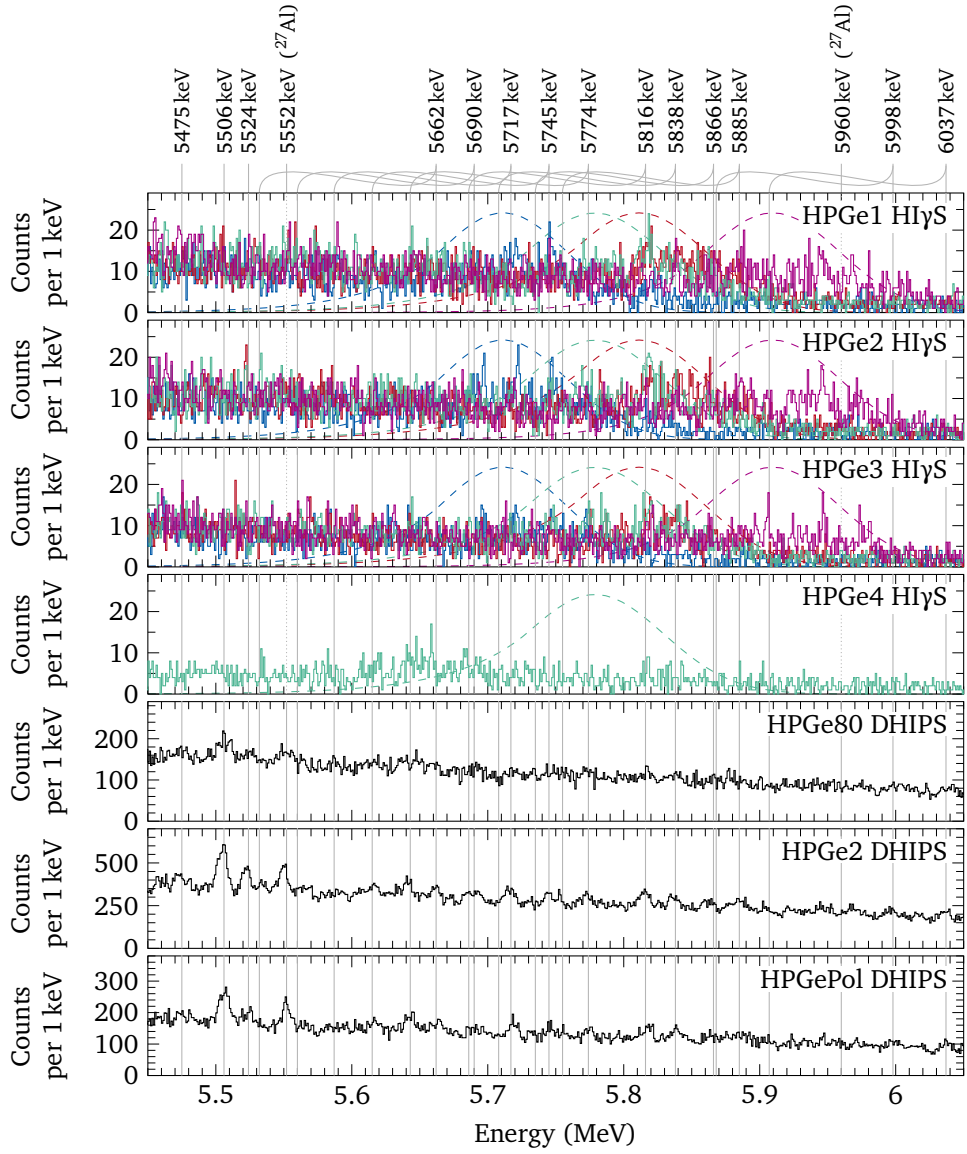

Figure 2.11: DHIPS and HIγS ^{150}Nd HPGe spectra for 5.5 MeV to 6.0 MeV.

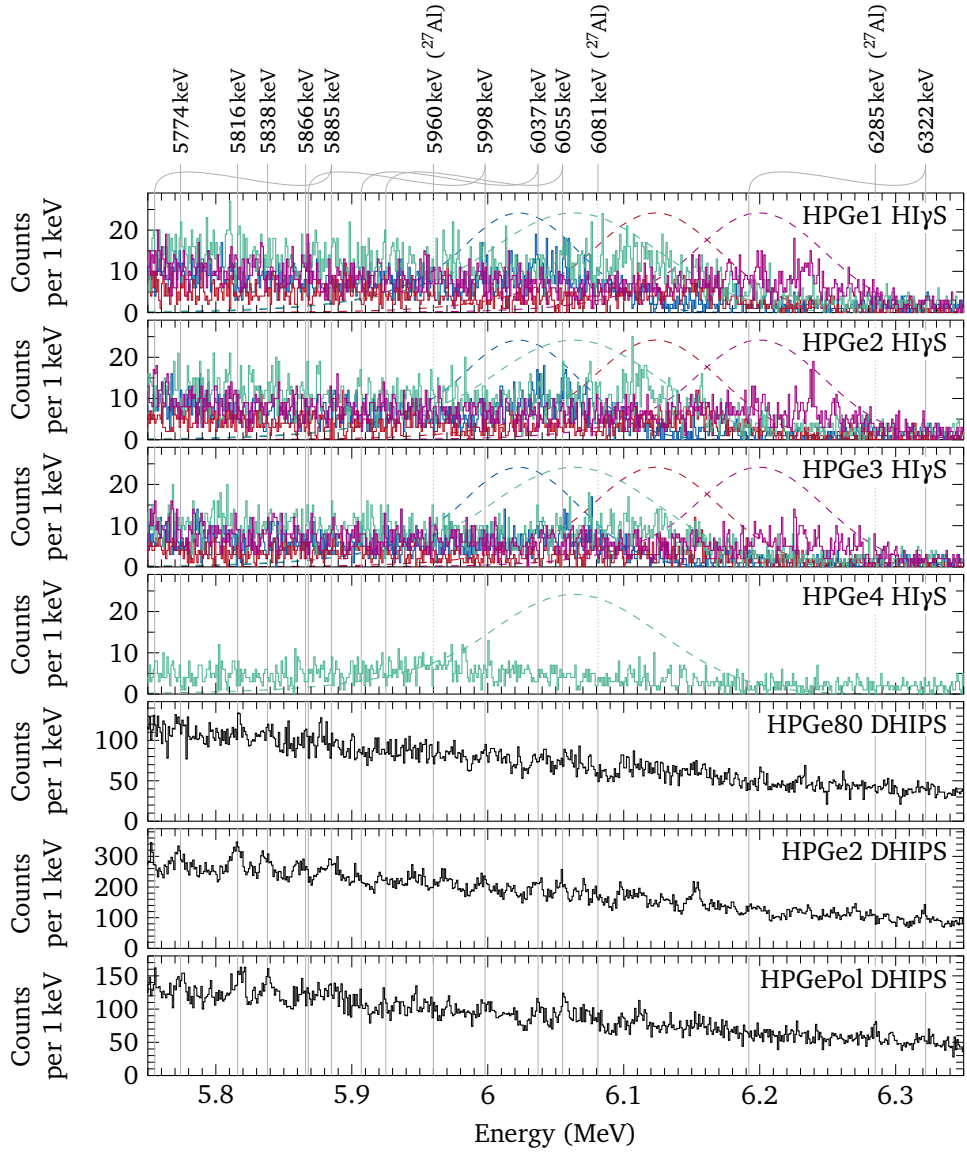

Figure 2.12: DHIPS and HIγS ^{150}Nd HPGe spectra for 5.8 MeV to 6.3 MeV.

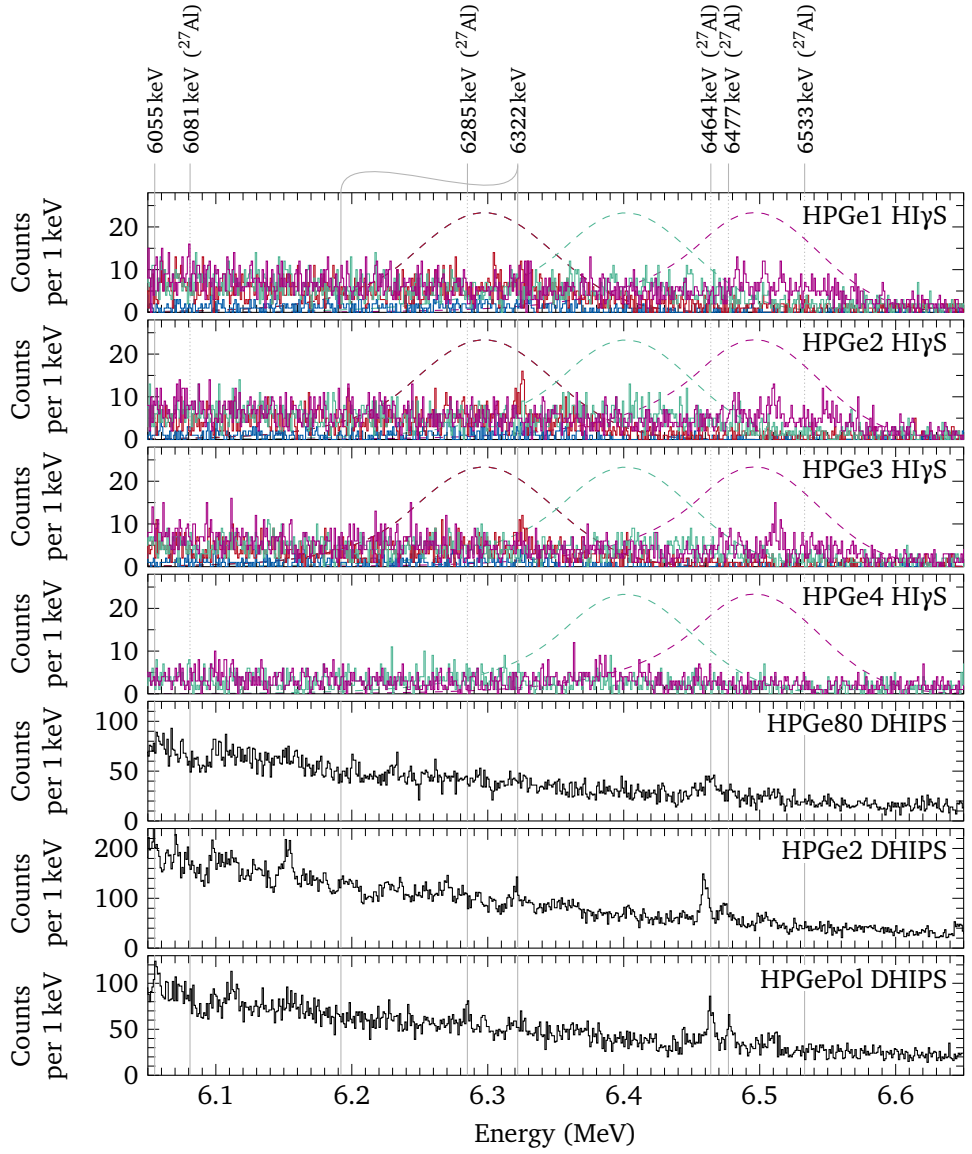

Figure 2.13: DHIPS and HIγS ^{150}Nd HPGe spectra for 6.1 MeV to 6.7 MeV.

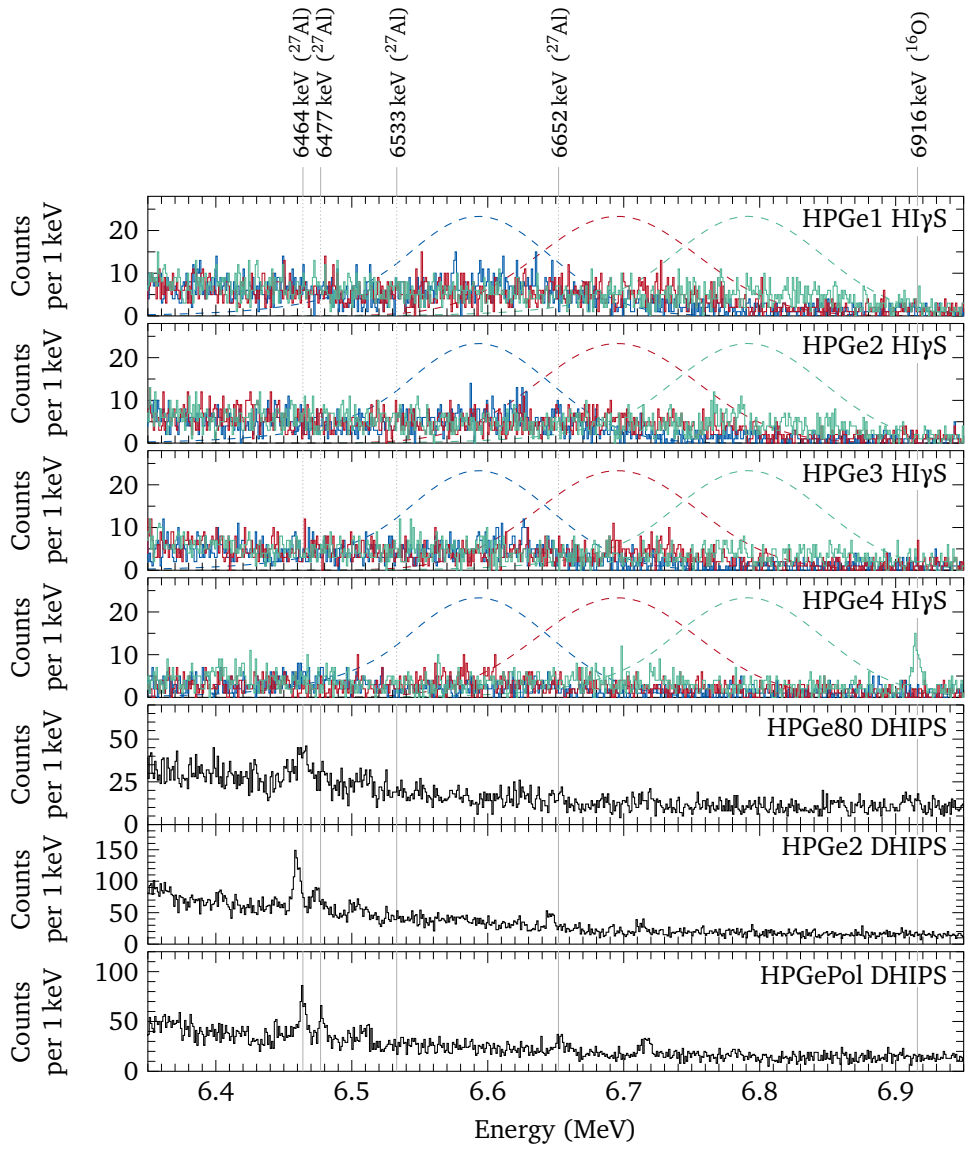

Figure 2.14: DHIPS and HIγS ^{150}Nd HPGe spectra for 6.4 MeV to 7.0 MeV.

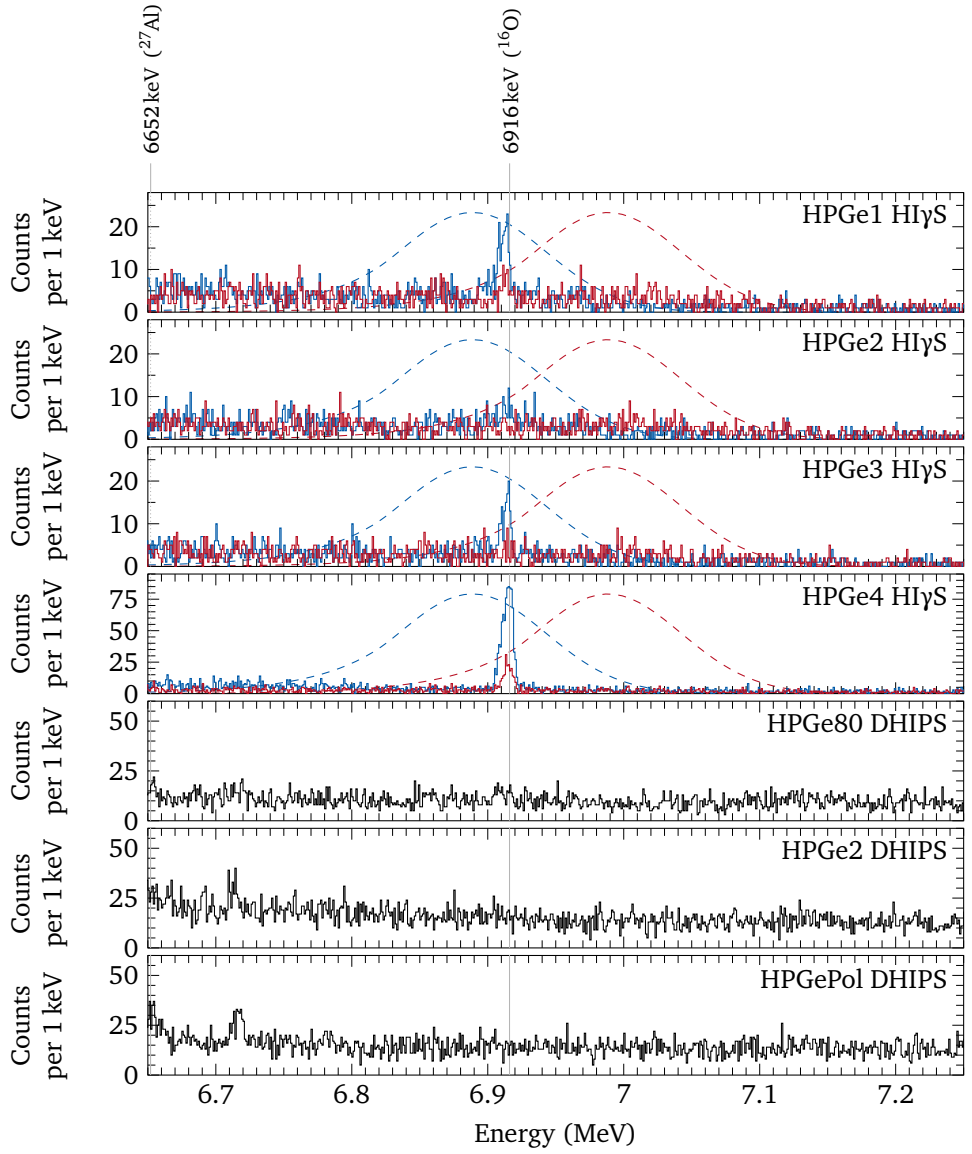

Figure 2.15: DHIPS and HIγS ^{150}Nd HPGe spectra for 6.7 MeV to 7.3 MeV.